AWARD NUMBER: W81XWH-16-C-0219

TITLE: Smartphone Enabled Point-of-care Diagnostics for Operationally Significant Pathogens

PRINCIPAL INVESTIGATOR: Dr. Ashutosh Chilkoti

CONTRACTING ORGANIZATION: Duke University
                                                         Durham, NC 27708-4677

REPORT DATE: October 2017

TYPE OF REPORT: Annual

PREPARED FOR: U.S. Army Medical Research and Materiel Command
                              Fort Detrick, MD 21702-5012

DISTRIBUTION STATEMENT: Approved for Public Release;
                                              Distribution Unlimited

The views, opinions and/or findings contained in this report are those of the author(s) and should not be construed as an official Department of the Army position, policy or decision unless so designated by other documentation.

REPORT DOCUMENTATION PAGE

Public reporting burden for this collection of information is estimated to average 1 hour per response, including the time for reviewing instructions, searching existing data sources, gathering and maintaining the data needed, and completing and reviewing this collection of information. Send comments regarding this burden estimate or any other aspect of this collection of information, including suggestions for reducing this burden to Department of Defense, Washington Headquarters Services, Directorate for Information Operations and Reports (0704-0188), 1215 Jefferson Davis Highway, Suite 1204, Arlington, VA 22202-4302. Respondents should be aware that notwithstanding any other provision of law, no person shall be subject to any penalty for failing to comply with a collection of information if it does not display a currently valid OMB control number. **PLEASE DO NOT RETURN YOUR FORM TO THE ABOVE ADDRESS.**

1. REPORT DATE	2. REPORT TYPE	3. DATES COVERED
October 2017	Annual	28 Sept 2016 – 27 Sept 2017

4. TITLE AND SUBTITLE
Smartphone Enabled Point-of-care Daignostics for Operationally
Significant Pathogens

5a. CONTRACT NUMBER

5b. GRANT NUMBER
W81XWH-16-C-0219

5c. PROGRAM ELEMENT NUMBER

6. AUTHOR(S)
Ashutosh Chilkoti, PhD
Michael Gunn, MD

E-Mail: ashutosh.chilkoti@duke.edu, michael.gunn@duke.edu

5d. PROJECT NUMBER

5e. TASK NUMBER

5f. WORK UNIT NUMBER

7. PERFORMING ORGANIZATION NAME(S) AND ADDRESS(ES)
Duke University
2200 W Main Street, Ste 710
Durham, NC 27708-4677

8. PERFORMING ORGANIZATION REPORT NUMBER

9. SPONSORING / MONITORING AGENCY NAME(S) AND ADDRESS(ES)

U.S. Army Medical Research and Materiel Command
Fort Detrick, Maryland 21702-5012

10. SPONSOR/MONITOR'S ACRONYM(S)

11. SPONSOR/MONITOR'S REPORT NUMBER(S)

12. DISTRIBUTION / AVAILABILITY STATEMENT
Approved for Public Release; Distribution Unlimited

13. SUPPLEMENTARY NOTES

14. ABSTRACT
We developed a novel high-throughput screen in microarray format that identifies optimal pairing of antibody pairs, which led to successful identification of optimal antibody reagents for Ebola having excellent sensitivity. We have identified 24 highly promising clones for antibody reagents used for detecting Salmonella. We successfully developed an approach for "self-calibrating" assay chips that correlate fluorescence intensities to the true known concentration of spiked Ag in serum. We have also identified an optimal strategy for labeling our reagents that is well-suited for our portable assay reader. Furthermore, we have developed 3 redundant designs for our ruggedized, portable reader in case of primary device failure. For assay cassettes, we have devised a simple, low-cost chip that encases all reagents and test components in a user-friendly format. Finally, we devised a development strategy for a smartphone app that automates assay readout.

15. SUBJECT TERMS
Nanoscale, nonfouling, polymer brush, inkjet printing, point of care, Ebola, Salmonella, antibody, antigen, smartphone, diagnostics, single-chain variable fragment, phage

16. SECURITY CLASSIFICATION OF:			17. LIMITATION OF ABSTRACT	18. NUMBER OF PAGES	19a. NAME OF RESPONSIBLE PERSON USAMRMC
a. REPORT	**b. ABSTRACT**	**c. THIS PAGE**	Unclassified	28	**19b. TELEPHONE NUMBER** *(include area code)*
Unclassified	Unclassified	Unclassified			

TABLE OF CONTENTS

I. INTRODUCTION

Enteric fever is caused predominantly by infection with Salmonella serovars Typhi (Typhoid Fever) or Paratyphi (Paratyphoid Fever). These infections represent a significant global health problem, causing 25 million illnesses and over 200,000 deaths each year. Additionally, at the time this proposal originally was drafted, over 25,000 cases of Ebola virus (EBOV) infection occurred with nearly 11,000 fatalities. For enteric fever EBOV infection, the timely initiation of antibiotic therapy or supportive care (respectively) can significantly decrease morbidity and mortality. Current diagnostic approaches require specialist facilities and trained personnel, and are relatively slow, potentially delaying life-saving therapy. We have developed a point-of-care test (POCT) platform—the "D4 assay"—that uses one drop of blood and requires no mixing of reagents, power, or equipment other than a smart phone. The D4 POCT consists of a nanoscale "nonfouling" — protein and cell resistant— poly(oligoethylene glycol methyl ether methacrylate) (POEGMA) brush coated glass chip that contains two types of printed microspots: "stable" microspots of capture antibodies (cAb) and "soluble" microspots of fluorophore labeled detection antibodies (dAb) (Fig. 1). The D4 assay is so named because it has four steps: first, fingerstick blood is dispensed on the chip, which dissolves the soluble spots of fluorescently labeled detection antibodies (dAbs), which diffuse and bind to their respective analyte-bound capture antibody (cAb) spots and generate a quantifiable optical signal that is detected by a custom fluorescence detector that attaches to a
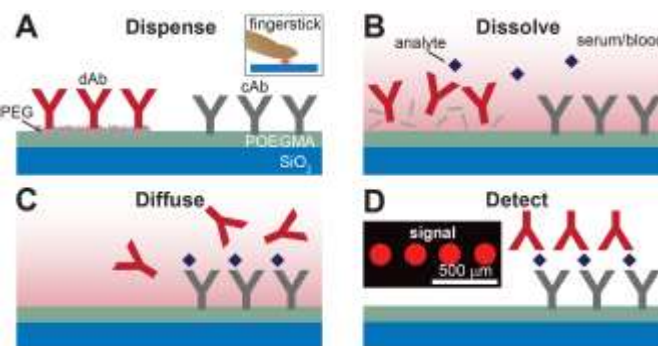
Fig 1: D4 (Dispense, Dissolve, Diffuse, Detect) assay on POEGMA**.**

smart phone. The images of fluorescent spots captured by the smart phone camera are converted to analyte concentration by a phone app. The D4 POCT is ideally suited for far forward special operations field settings for the following reasons: it is far more sensitive than existing immunoassays, test cassettes cost pennies and are stable at room temperature for months, and is read with a smartphone, generating data with minimal sample processing and operator training. As described in greater detail in Section III below, the **overall goal** of this project was to develop a D4 POCT platform capable of early diagnosis of infectious pathogens of operational significance.

II. KEYWORDS

Nanoscale, nonfouling, polymer brush, inkjet printing, point of care, Ebola, Salmonella, antibody, antigen, smartphone, diagnostics, single-chain variable fragment, phage

III. ACCOMPLISHMENTS

A. Major Goals of the Project
The overall goal of this project is to develop a D4 POCT platform for blood markers of infectious diseases for use by special operations' personnel in any region of the world. Specifically, the proposed work is expected to produce a portable, ruggedized D4 POCT that for timely

identification of infection with Salmonella serovars and Ebola virus (EBOV). This diagnostic is based on the detection of circulating Salmonella and Ebola antigens (Ags) for early and rapid diagnosis of disease. This in turn would allow rapid interventions before reaching critical illness. Specifically, the technical objectives (TOs) are shown below, along with the percentage of completion:

TO#	Description	Completion
1	Generate a panel of EBOV-specific capture and detection Abs	95%
2	Generate a panel of S. enterica-specific capture and detection Abs	50%
3	Ab integration and technology optimization of D4 POCT	50%
4	Validation of EBOV D4 POCT using blood samples obtained from EBOV-infected primates	0%
5	Validation of S. enterica D4 POCT using blood and serum samples form Salmonella-infected patients	10%

Significant Changes in Methods
1. Although not part of our original proposal, we modified our procedures to include the conversion of scFv clones to an scFV-Fc format. This markedly accelerated our ability to identify clones that display the optimum binding characteristics. We successfully developed a methodology to perform this conversion in a high-throughput manner.
2. We developed a novel high-throughput screen in microarray format that both identifies paired capture and detection Abs, and identifies those Ab pairs that function with the highest sensitivity. This methodology was applied to identify the best Ab pair for EBOV.
3. For Salmonella, we discovered that flagellin will not be an informative marker for S. Paratyphi. This appears not to be true for S. Thyphi, but we will need to confirm this ourselves. Thus we proceeded to identify numerous highly specific clones for both S. Thyphi flagellin and Vi Ag. These are currently being converted to scFv-Fcs, which will be subjected to the same high-throughput screen used for EBOV. If S. Thyphi Vi Ag works well, we will use it for S. Paratyphi.

B. Accomplishments Under These Goals
Major Activities & Specific Objectives
Over the past funding year, the **major activities** of the project revolved around generation of highly-specific assay reagents and optimization of the D4 POCT platform. The **specific objectives** of the project that were pursued in parallel during the funding period (which correspond to the TOs in the original proposal) were as follows:
1. Generate a panel of EBOV-specific capture and detection Abs
2. Generate a panel of S. enterica-specific capture and detection Abs
3. Ab integration and technology optimization of D4 POCT

Significant Results & Key Outcomes
Objective 1: Generate a panel of EBOV-specific capture and detection Abs.
After screening for hundreds of individual scFv clones for binding to sGP in ELISA assays, we ultimately identified several dozen unique sGP-binding clones. From these, we selected 28 unique sGP-binding clones for further analysis. We even identified some that bind well to EBOV, but not Sudan virus, sGP, allowing us to distinguish these two strains. Because of the large number of

sGP-binding scFv clones we identified above, we decided to develop a novel high-throughput screen in microarray format that would: 1) identify paired capture and detection Abs; 2) identify those Ab pairs that detect sGP with the highest sensitivity; and 3) include use of the D4 assay format to ensure that the identified clones will function well in our final assay format. This high-throughput screening approach proved to be very successful, as demonstrated with EBOV (described below).

By applying our screening method, we successfully identified the sGP-binding scFv clone that would clearly function best as a capture Ab (clone A1F3-1). We also identified multiple detection Abs that effectively paired with this capture Ab. These clones are shown below in Fig. 1, and highlighted in green boxes. Importantly, these detection Abs include several that detect both the Zaire and Sudan strains of Ebola virus and one that is specific for the Zaire strain, which will allow us to develop an assay that can distinguish infection by these two strains. In addition, in titration assays, these Ab pairs could detect sGP with a sensitivity of less than 1 ng/ml. The dose-response behavior for each of these Ab pairs in D4 format is shown in Fig. 1, with each pair already showing excellent sensitivity (sub-nanogram/mL) and dynamic range in D4 assay format. We converted the best clones into full length IgGs, which showed improved performance in ELISAs. We are in the process of testing these in the D4 format.

Although not part of our original proposal, we modified our procedures to include the conversion of scFv clones to an scFV-Fc format. This markedly accelerated our ability to identify clones that display the optimum binding characteristics. In support of this change, we have now
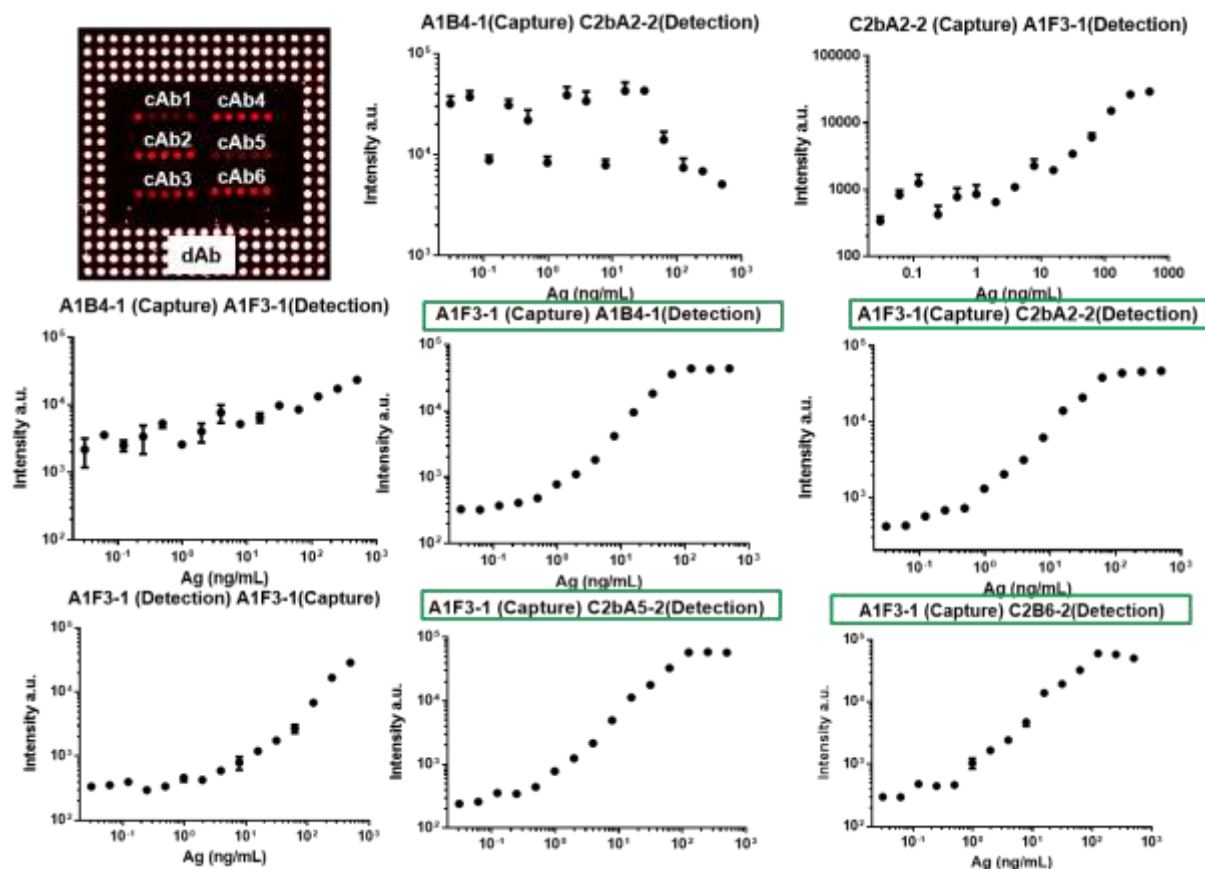

Fig. 1: EBOV sGP D4 assay. Results of Ab pair matching in D4 format. <u>Best performing pairs indicated with green boxes</u>.

successfully developed a methodology to perform this conversion in a high-throughput manner. One issue we are dealt with is the exact format in which scFv-Fc constructs are generated. For EBOV, we originally used an IgG1 Fc construct. However, purification of the scFv-Fcs produced proved to be suboptimal. We <u>resolved</u> this issue by changing our expression construct to include an IgG2a Fc segment, which enabled superior purification efficiency.
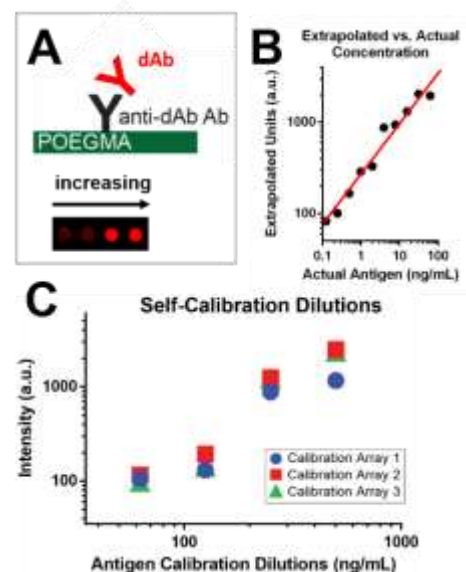
<u>Objective 2: Generate a panel of S. enterica-specific capture and detection Abs.</u>
We generated Ab pairs specific for S. Paratyphi flagellin, and these were shown to work well in the D4 assay. However, in studies that were not part of our actual proposal, we determined that significant levels of S. Paratyphi flagellin is not detected in the serum of individuals infected with this organism. We thus sought to develop Ab pairs specific for Vi capsular polysaccharide in parallel, and we are currently completing our analysis of both targets target for S. Typhi. To date, we have identified 24 unique flagellin or Vi binding scFv clones for further analysis. The conversion of anti-flagellin clones to the scFV-Fc format has now been completed. These Abs have been slated for testing using the high-throughput Ab pair matching scheme in microarray format described above, which was highly effective for EBOV. We are in the process of converting Vi binding scFv clones to the scFV-Fc format.

<u>Objective 3: Ab integration and technology optimization of D4 POCT.</u>
We have successfully identified the optimal capture and detection spot placement on D4 chips. Chips utilizing a design incorporating capture spots printed within concentric rings of detection reagents showed optimal performance compared to other array layouts. This task was completed ahead of schedule.

In our original proposal we sought to print spots of Ag onto the polymer surface to act as "self-calibrating spots". Unfortunately, we observed that not all Ags immobilized as well as Abs onto the polymer surface. This is likely due to the diversity in size and structure of different Ags. To address this issue, we pursued 3 parallel strategies for constructing self-calibrating D4 assay chips: (a) printing spots of pre-bound Ab-Ag complexes as a dilution series (b) printing dilution series of anti-dAb Abs and (c) printing printing Ab-Ag chimeras, in which Ags are expressed with linker from Ab scaffolds. These approaches are

Fig. 2: Self-calibrating chip – anti-dAb Ab. (A) Schematic of calibration. **(B)** Extrapolated values vs. known values shows linear relationship. **(C)** Chip-to-chip consistency of calibration spots.

motivated by the observation that Abs possess the ideal size (~150 kD) and physiochemical characteristics for noncovalent immobilization in the polymer brush surface. Remarkably, each method showed effective immobilization and activity. Based on the results of our experiments— along with considering the cost per assay—we downselected our final approach to strategy (b)— printing anti-dAb Abs as calibration spots (Fig. 2A). We used this approach to correlate fluorescence intensities to the true known concentration of spiked Ag in serum (Fig. 2B). Furthermore, correcting intensities by calibration spots reduces chip-to-chip variation (Fig. 2C).
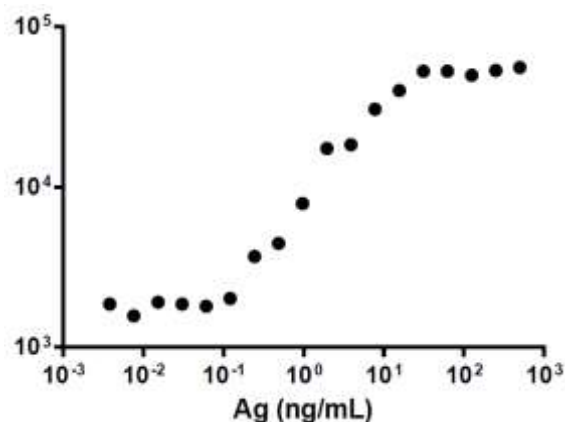
In our work towards ruggedizing and further miniaturizing the D4 detector, we recognized that the optics were not sufficiently sensitive for visualizing organic fluorophores to the extent needed for our application. To address this, we elected to switch to quantum dot probes (which are several orders of magnitude brighter) as reporters. Quantum dot reporters are not susceptible to bleaching and show favorable optical characteristics (e.g. large Stokes shift between excitation and emissions wavelengths, large quantum efficiency). We pursued 2 main strategies for conjugating dAbs to quantum dot reporters: (1) covalent conjugation by EDC-NHS coupling and (2) coupling of streptavidin-conjugated quantum dots to biotinylated dAb. Based on testing results, we downselected our choice down to strategy (2)—streptavidin-biotin conjugates. Using this approach, we achieve good assay sensitivities in D4 (sub-nanogram/mL) (Fig. 3).

Fig 3: Analytical performance of D4 chips utilizing streptavidin-QD/biotin-dAb conjugates as labeling strategy, showing sub-nanogram/mL sensitivity.

For the portable detector, we have embedded redundancy into our approach by developing 3 detector embodiments. These designs are displayed in Fig. 4, which shows the "handheld", "flashlight-compatible", and "pocket" versions of the detector. All 3 models are rugged and portable. This approach was adopted based on SOCOM input, wherein redundancy in readout provides backup plans in case of primary device failure. We continue to iterate cycles of 'design-test-modify' for these detector embodiments in parallel with our assay development efforts.

Fig. 4: Ruggedized portable detector with redundancy in design. Handheld, flashlight, and pocket embodiments shown. Representative array images with handheld and flashlight designs shown.

We continue to make progress in developing a D4 with sealed chip architecture. As displayed in Fig. 5, we have devised a simple, low-cost microfluidics chip that is driven to completion by capillary action. The chip encases all reagents and test components in a user-friendly format. Fabrication is also simple—chips and channel features are laser cut directly on a plexiglass sheet, and then adhered directly to a POEGMA-coated glass surface containing assay reagents. Since the chip is capillary-driven, no power, electronics, nor pumps/valves are required for chip operation other than applying liquid to the chip.

Finally, we have initiated development of the smartphone app to quantify spot intensities. This task will be carried out at by a team at Duke. Our strategy for software development involves the use of Python code because it is free, open-source, well-documented, and highly versatile. These factors allow for a more agile development cycle and more precise control of our raw data; the versatility of Python's OpenCV open-source computer vision software package has more intuitive image processing algorithms than our current proprietary software.

C. Opportunities for Training and Professional Development

This project provides an exceptional training opportunity for three individuals – Margaret Lund (research associate), Daria Semeniak (PhD student), and Daniel Joh (MD-PhD student). By working with other senior members of the laboratory, they gained proficiency in a wide range of skills. Examples include polymerization of POEGMA by SI-ATRP, characterization of the POEGMA brush on glass, inkjet printing of the microarrays, assay optimization, and assembly of cassettes/detectors of the "D4" point-of-care test (POCT).

Fig. 5: Self-calibrating chip. (A-B) Sealed, self-clearing, assay chip made from cheap, rugged materials (laser-cut plastic & glass). Images immediately after addition of sample (S; whole serum) and at conclusion of assay. Wash (W) and sample *colored with food coloring for ease of visualization*. Assay automatically timed and goes to completion after addition of serum, based on capillary action.
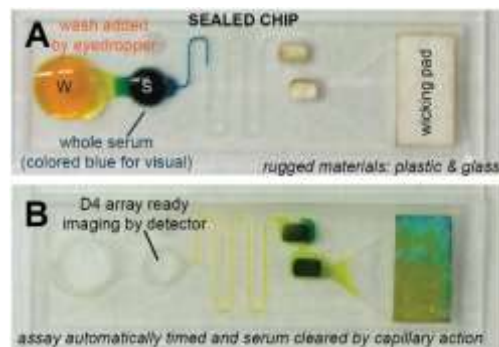
D. Dissemination of Results to Communities of Interest

We made our research accessible and comprehensible to the general community by organizing lab tours for incoming college students at Duke.

E. Plans During Next Reporting Period

In the **short-term**, we plan to pursue several tasks which are continuations of the 3 Technical (Specific) Objectives outlined above. With respect to Ab development, for Ebola we will first confirm the performance of our anti-sGP IgGs in the D4 format using recombinant sGP spiked into human serum. This assay will then be optimized by varying Ab concentrations and incubation times. For S. Typhi, we are in the process of testing individual Ab clones in the D4 format using recombinant flagellin. Once this is completed, we will subject these Abs to Capture/Detection Ab pairing using our novel high-throughput matching procedure. Optimal pairs will be converted to IgGs an validated in the D4 format using recombinant flagellin. The assay will then be optimized and validated against serum obtained from S. Typhi infected humans. Our anti-S. Typhi Vi Ab clones are currently being converted to scFv-Fc molecules. Once this is accomplished, these Abs will be tested and validated as described for the flagellin Abs above. If the anti-S. Typhi Vi Ab clones prove to function well, we will generate, test, and validate anti-S. Parahyphi Vi Ab clones in a manner used for the anti-S. Typhi Vi Ab clones. As candidates for assay reagents for each pathogen become available and finalized, we will fully characterize assay performance (including matrix effects) to downselect assay reagents that will be used for pre-clinical testing. These assay chips will also be iteratively optimized in conjunction with the 3 detector designs shown in Fig. 4 to ensure compatibility. We are also completing a preliminary algorithm for the smartphone app. The app will be capable of automatic identification of microspot arrays. It will also discriminate between capture spots versus detection spots, and then quantify capture spot intensities for the user. This will all occur in an automated manner.

In the **long-term**, once final assay reagents are chosen and optimized individually on the chip, we will then combine them in multiplex format. The goal is to complete integration and optimization of the multiplex D4 assay by month 9 of year 2. Months 9-10 will be occupied by testing each assay with simulated blood samples and comparing results to ELISAs produced in-house. The results will be interpreted by an interclass correlation (ICC) between our measure versus ELISA. Our hypothesis is that this sample size will lead to an ICC above 0.8, but the greater utility will be to assess the confidence interval of the ICC, which in samples this size will have bounds of ~+0.10. Bland-Altman methods will assess the degree of bias between the two measures. Next, during

Months 11-12 of the funding period, we will test the ability for the D4 POCT to predict group membership (infection vs. no infection) in patient (Salmonella) specimens from Oxford and primate (EBOV) specimens in the BSL-4 facility in Galveston. To interpret the results, we will use logistic regression to assess the degree of segregation measured by area under the curve (AUC). We anticipate that our test will yield an AUC > 0.8.

IV. IMPACT

A. Impact on development of the principal disciplines of the project

If successful, this project will have major **clinical impact** by introducing an affordable, accurate blood test for early and accurate point-of-care detection of S. enterica and EBOV infection, potentially prior to the onset of symptoms. Such technology has life-saving potential for special operations personnel by allowing clinical interventions before fulminant disease progression.

This project also has potential to make a major **scientific impact**, as successful demonstration in human and animal cohorts will provide prima facie validation of novel early markers for S. enterica serovars and Ebola virus. This has practice-altering implications since early markers for these diseases are urgently needed.

As a result of this project, we developed a novel high-throughput screen in microarray format that both identifies paired capture and detection Abs, and identifies those Ab pairs that function with the highest sensitivity. This methodology was successfully applied to identify the best Ab pair for EBOV. This approach is broadly applicable to any situation where Ab pair matching is required, and is thus likely to have a **major impact** specifically in the field of immunoassay development. Our goal is to complete a manuscript summarizing the techniques and our findings in a peer-reviewed journal.

B. Impact on Other Disciplines & Society

D4 platform can target any analyte for which clinical reagents (such as antibodies) are available. Therefore, the approach described in this application is ideal for developing rapid and accurate point-of-care tests for the diagnosis and management of most diseases of operational and global health significance. The endstate is being able to provide an array of D4 cassettes for specific regions of the world, i.e., an array of chips focused on the most important infectious agents on the African continent, or any other particular region of the world where military or global health personnel are deployed. This work also introduces a highly robust, generalized system for the rapid development, validation, translation, and scaling of biomarker tests with potential application to other diseases in need for early markers, in a manner not available to prior researchers in the field. This development would have large impact on military operations and global health applications. Examples include rapid deployment of tests for civilian disaster scenarios, bioterrorism, and population-based validation of novel blood tests for diseases in desperate need of new diagnostic options (e.g. cancer screening).

C. Impact on Technology Transfer

Nothing to report

V. CHANGES & PROBLEMS

A. Changes in Approach and Reasons for Change

Conversion from scFv to scFv-Fc. Although not part of our original proposal, we modified our procedures to include the conversion of scFv clones to an scFV-Fc format. This markedly accelerated our ability to identify clones that display the optimum binding characteristics. We successfully developed a methodology to perform this conversion in a high-throughput manner.

Salmonella Ags. For Salmonella, we discovered that flagellin will not be an informative marker for S. Paratyphi B infection. Thus, for S. Typhi, we proceeded to identify numerous highly specific clones for both flagellin and Vi Ag. These are currently being converted to scFv-Fcs, which will be subjected to the same high-throughput screen used for EBOV. If Vi clones function well for S. Typhi, we will use this strategy for S. Paratyphi.

B. Actual or Anticipated Problems or Delays and Actions to Resolve Them

Problem 1: In studies that were not part of our actual proposal, we determined that significant levels of S. Paratyphi flagellin are not detected in the serum of individuals infected with this organism.
Solution: We identified Vi capsular polysaccharide as an alternative targt, which we will evaluate once we have completed our analysis of this target for S. Typhi.

Problem 2: Our original plan was to directly print calibration gradients of Ags onto POEGMA as internal calibration spots. However, we observed that directly printed protein Ags (typically smaller than Abs) do not always non-covalently immobilize as effectively as printed Abs. This led to some spots of printed Ag to appear quite dim after running the assay because of their poor immobilization.
*Solution***:** To overcome this obstacle, we explored 3 candidate approaches, based on the observation that that Abs possess the ideal size (~150 kD) and physiochemical characteristics for noncovalent immobilization in the POEGMA brush surface. These approaches were: (1) printing spots of pre-bound Ab-Ag complexes as a dilution series (2) printing dilution series of anti-dAb Abs and (3) printing Ab-Ag chimeras using methods developed in our laboratory, in which Ags are expressed with linker from Ab scaffolds. The results of our experiments allowed us to downselect our final strategy to strategy (2)—printing anti-dAb Abs as calibration spots. We used this approach to correlate fluorescence intensities to the true known concentration of spiked Ag in serum. Furthermore, correcting intensities by calibration spots reduces chip-to-chip variation.

Problem 3: In our work towards ruggedizing and further miniaturizing the D4 detector, we recognized that portable optics were not sufficiently sensitive for visualizing spots of organic fluorophores.
*Solution***:** We performed parallel experiments using quantum dot probes as reporters instead of organic fluorophores. This approach was chosen since they are several orders of magnitude brighter than organic fluorophores, with much narrower emission wavelengths. Furthermore, quantum dots that emit in the visible range have zero spectral overlap between excitation and emission wavelengths (a large "Stokes shift"), further simplifying the detection optics. We pursued 2 main strategies for conjugating dAbs to quantum dot reporters: (1) covalent conjugation by EDC-NHS coupling and (2) coupling of streptavidin-conjugated quantum dots to biotinylated dAb. Based on testing results, we downselected our choice down to strategy (2)—streptavidin-biotin conjugates. Using this approach, we achieve good assay sensitivities in D4 (sub-nanogram/mL).

Problem 4: For EBOV, we used an IgG1 Fc construct. However, purification of the ScFv-Fcs produced proved to be suboptimal.
*Solution***:** We are converted our expression construct to include an IgG2a Fc segment which successfully provided superior purification efficiency.

C. Changes that Had Significant Impact on Expenditures

Nothing to report

D. Significant Changes in Use or Care of Human Subjects, Vertebrate Animals, Biohazards, and/or Select Agents

Nothing to report

VI. PRODUCTS

A. Publications, conference papers, and presentations

Journal Publications

Citation	Status	Acknowledgement of Support?
Joh DY, Hucknall AM, Wei Q, Mason KA, Lund ML, Fontes CM, Hill RT, Blair R, Zimmers Z, Achar RK, Tseng D, Gordan R, Freemark M, Ozcan A, Chilkoti A. Inkjet-printed point-of-care immunoassay on a nanoscale polymer brush enables subpicomolar detection of analytes in blood. *Proc Natl Acad Sci U S A*. 2017;114(34):E7054 E7062.	Published	yes

VII. PARTICIPANTS & OTHER COLLABORATING ORGANIZATIONS

A. Individuals on the Project

Name: Ashutosh Chilkoti
Project Role: PI
Research Identifier: 0000-0002-1569-2228 (ORCID ID)
Nearest person month worked: 1
Contribution to project: Contact PI responsible for fiscal and administrative management of the project. Responsible for engineering and assay development efforts, which includes overseeing fabrication and analytical equipment needed to design, build and test the components of the D4
Funding Support:

Name: Margaret Lund
Project Role: Associate in Research
Research Identifier: N/A
Nearest person month worked: 4
Contribution to project: Participated in all aspects of D4 assay fabrication (SI-ATRP of polymer coatings, inkjet printing, cassette assembly, testing/optimization, etc.); assembly and optimization of the detector
Funding Support:

Name: Daria Semeniak
Project Role: Graduate Student
Research Identifier: N/A
Nearest person month worked: 1

Contribution to project: Participated in all aspects of D4 assay fabrication (SI-ATRP of polymer coatings, inkjet printing, cassette assembly, testing/optimization, etc.); assembly and optimization of the detector
Funding Support:

Name: Daniel Joh
Project Role: Graduate Student
Research Identifier: N/A
Nearest person month worked: 1
Contribution to project: Participated in all aspects of D4 assay fabrication (SI-ATRP of polymer coatings, inkjet printing, cassette assembly, testing/optimization, etc.); assembly and optimization of the detector
Funding Support: Duke Medical Science Training Program (MSTP) T32 Funding

Name   Michael Gunn
Project Role: Co-PI
Research Identifier: 0000-0003-4602-0667 (ORCID ID)
Nearest person month worked: 1
Contribution to project: Responsible for overseeing efforts of generating high-affinity recombinant antibodies for integration into the D4 POCT.
Funding Support:

Name: Barbara Lipes
Project Role: Research Associate
Research Identifier: 0000-0003-1195-9463 (ORCID ID)
Nearest person month worked: 2
Contribution to project: Responsible for generating high-affinity recombinant antibodies using single-chain Ab (scFv) phage display technology. Also responsible for animal work required to harvest spleens of immunized mice and eventually screen for high affinity Ag-specific scFv clones based on their binding characteristics
Funding Support:

B. Changes in Other Support

Dr. Ashutosh Chilkoti
1. *Grants Ended*: North Carolina Biotechnology Center grant—ended 9/30/17; Pfizer grant—ended 9/11/17
2. *New Grants*: USAMRAA SO150005, W81XWH-16-C-0219; NIH, 1R01GM123542; Dr. Reddy's Laboratories—2 new grants (CIS-Platinate and Paclitaxel); NIH, UG3CA211232; NIH, 1R21CA218940; NSF, 1729671; USAMRMC, DM160400

Dr. Michael Gunn
Nothing to report

C. Other organizations were involved as partners

Organization Name: Immucor Inc.

Location of Organization: Norcross, GA
Partner's contribution to the Project**:** Collaboration, in-kind support, facilities

Organization Name: Oxford University (Pollard Laboratory)
Location of Organization: United Kingdom
Partner's contribution to the Project**:** Collaboration

Organization Name: University of Texas Medical Branch at Galveston (Geisbert Laboratory)
Location of Organization: Galveston, TX
Partner's Contribution to the Project**:** Collaboration

VIII. SPECIAL REPORTING REQUIREMENTS

A. Quad Chart
See Section IX (Appendices) below

IX. APPENDICES

Attached as appendices

1. Updated quad chart
2. Copy of journal article which acknowledges support from USSOCOM (*Proc Natl Acad Sci U S A*. 2017;114(34):E7054 E7062.)
3. Complete summary of Other Support for Dr. Chilkoti

Smartphone POC Diagnostics
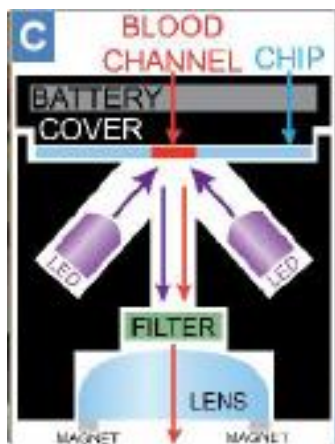
Far Forward Decision Support Tools

Timeline

Activities	Year 1	Year 2
TO1: EBOV Ab Reagents		
TO2: Salmonella Ab Reagents		
TO3: Optimization of D4 POCT		
TO4: Clinical Validation - EBOV		
TO5: Clinical Validation - Salmonella		

The So What

- **SOF Medics operating in an austere operational environments need a decision support tool to assist with diagnosing pathogens and infectious diseases**
- **Diagnostic technology is broadly applicable to target any analyte where antibody pairs are available can be applied**

Benefits

- **Simple, handheld, battery-operated instrument that is read with a smart phone and analyzes samples obtained from blood**
- **High sensitivity and specificity equals low false positive rate providing an accurate answer and supporting medical decisions**

Inkjet-printed point-of-care immunoassay on a nanoscale polymer brush enables subpicomolar detection of analytes in blood

Daniel Y. Joh[a,1], Angus M. Hucknall[a,1,2], Qingshan Wei[b], Kelly A. Mason[c], Margaret L. Lund[a], Cassio M. Fontes[a], Ryan T. Hill[a], Rebecca Blair[a], Zackary Zimmers[a], Rohan K. Achar[a], Derek Tseng[b], Raluca Gordan[d], Michael Freemark[c], Aydogan Ozcan[b], and Ashutosh Chilkoti[a,2]

[a]Department of Biomedical Engineering, Pratt School of Engineering, Duke University, Durham, NC 27708; [b]Electrical Engineering and Bioengineering Departments, Henry Samueli School of Engineering and Applied Science, University of California, Los Angeles, CA 90095; [c]Division of Pediatric Endocrinology, Department of Pediatrics, School of Medicine, Duke University, Durham, NC 27705; and [d]Center for Genomic and Computational Biology, Duke University, Durham, NC 27708

The ELISA is the mainstay for sensitive and quantitative detection of protein analytes. Despite its utility, ELISA is time-consuming, resource-intensive, and infrastructure-dependent, limiting its availability in resource-limited regions. Here, we describe a self-contained immunoassay platform (the "D4 assay") that converts the sandwich immunoassay into a point-of-care test (POCT). The D4 assay is fabricated by inkjet printing assay reagents as microarrays on nanoscale polymer brushes on glass chips, so that all reagents are "on-chip," and these chips show durable storage stability without cold storage. The D4 assay can interrogate multiple analytes from a drop of blood, is compatible with a smartphone detector, and displays analytical figures of merit that are comparable to standard laboratory-based ELISA in whole blood. These attributes of the D4 POCT have the potential to democratize access to high-performance immunoassays in resource-limited settings without sacrificing their performance.

nanoscale | nonfouling | polymer brush | inkjet printing | point of care

Diagnostic assessment of protein biomarkers plays an essential role in modern medical practice, and its availability has a considerable impact on clinical evaluation and decision making in human health and disease (1). Diagnostic biomarkers are not only used for identifying disease in individual patients but also for developing treatment strategies, tracking treatment response, monitoring recurrence, conducting clinical trials, and performing epidemiological analysis (2). However, shortages in sophisticated laboratory resources, highly trained personnel, and modern facilities (with clean water, cold storage, and reliable power) have hampered the discovery and use of diagnostic and therapeutic biomarkers in the developing world (3). The mainstay approach for sensitive and quantitative detection of protein biomarkers is the ELISA. In developed countries, highly sensitive ELISA and ELISA-like (4) sandwich immunoassay technologies are readily accessible in centralized facilities and are performed by trained operators or even automated to handle the multistep workflow. Much of the workflow is directed toward reducing biomolecular noise due to nonspecific binding of proteins and other components in complex biological fluids that lower signal-to-noise ratio (SNR). Depending on the assay, steps can include sample pre-processing, liquid transfer, blocking, incubation, and wash steps, in addition to data acquisition and analysis with bulky instrumentation. Taken together, these characteristics represent major barriers to obtaining highly sensitive quantitation of protein biomarkers in limited-resource settings (LRSs) (3). Furthermore, these barriers can also delay treatment, as test results from laboratory-based immunoassays may not always reach healthcare providers and patients in LRSs quickly enough to impact critical clinical decisions (1). To address these concerns, we sought to design and implement a broadly applicable protein

biomarker detection platform with performance comparable to resource- and personnel-intensive technologies such as ELISA while retaining the many attractive features (i.e., low cost, portability, and ease of use) of "passively" driven platforms such as lateral flow immunoassays (LFIAs) (5), paper-based diagnostics (PBDs) (6), and passive microfluidics (PMFs) (7).

In our previous work, we fabricated Ab-based microarrays on nanoscale poly(oligo(ethylene glycol) methacrylate) (POEGMA) polymer brushes that were capable of femtomolar detection of analytes directly from complex biological milieu (8). The Ab arrays were directly spotted onto POEGMA brushes that were grown from glass by surface-initiated atom transfer radical polymerization (SI-ATRP) (8, 9). The POEGMA's ability to resist nonspecific adsorption of proteins greatly improved SNR by reducing "biomolecular noise," translating to femtomolar limit of detection (LOD) of protein analytes even from whole blood and serum (8, 10, 11). The observation that Ab microarrays could be directly spotted and noncovalently immobilized onto POEGMA coatings, and that spots of Abs dried and captured within the POEGMA brush retained their activity even after drying and ambient storage, greatly simplified assay fabrication

Significance

Sensitive quantitation of protein biomarkers plays an important role in modern clinical decision making. This work introduces an inkjet-printed assay platform built on a nonfouling, nanoscale polymer brush, which eliminates nonspecific binding, the largest source of noise in surface-based assays. The assay goes to completion after adding a drop of blood (with no additional reagents or mixing), and the assay can be read with a smartphone-based detector. This technology is significant because it enables high-performance diagnostic testing in blood with minimal infrastructural requirements. Furthermore, its fully printed nature makes it highly customizable and thus broadly applicable to a wide range of diagnostic targets.

and subsequent storage of the microarrays. Significantly, the POEGMA-based microarrays also decreased the time needed to perform a sandwich immunoassay by eliminating the need for blocking steps and reducing the number of rinsing steps. Like most other immunoassays, however, this approach still required separate incubation steps for labeling with detection reagents to achieve a quantifiable signal. We therefore sought to build upon this body of work and the robust design concepts of existing "point-of-care test" (POCT) technologies to develop a quantitative and sensitive platform that stores all necessary reagents so that the assay is ready for readout following direct addition of blood or serum, while minimizing user intervention.

Here, we report a quantitative, self-contained, multiplexable immunoassay (the "D4 POCT") that stores all necessary capture and detection reagents "on-chip" in a dry state, shows durable stability without cold storage, and detects analytes with sensitivity comparable to ELISA directly from whole blood without sample preprocessing.

Results

Design of the D4 Immunoassay. The challenge we faced in redesigning an immunoassay on POEGMA brushes as a POCT, and one that is common to most POCTs, is how to spatiotemporally separate the capture and detection reagents, and how to time the precise sequence of events upon introduction of the analyte into the assay to yield a readout. Whereas recent work in PBDs that use highly innovative and robust sequential delivery techniques has been shown to be effective (12–15), our approach was to instead design a passive POCT that uses lateral diffusion in the polymer brush as the temporally programmable mixing principle. The architecture of the D4 assay consists of a glass chip with a ~50-nm-thick POEGMA coating that contains two types of microspots that are inkjet-printed on the polymer brush: "stable" spots of capture antibodies (cAb) and "soluble" spots of detection reagents (Fig. 1). Here, the capture and detection reagents are placed in very close proximity to one another (several hundred micrometers), unlike LFIAs in which reagents must travel larger distances. The detection reagent spots are soluble, as they consist of a mixture of fluorescently labeled detection Abs (dAbs) and excipient (such as PEG or trehalose) to enable dissolution upon liquid exposure (Fig. 1 *A* and *B*). The D4 assay is so named because of the chain of events that drive the assay to completion upon addition of a drop of blood (Fig. 1 *A–D*): (*A*) dispense blood onto chip, (*B*) dissolution of "soluble" detection reagent spots, (*C*) diffusion of analyte-bound dAb across surface and binding to respective cAb spots, and (*D*) detection of binding event by fluorescence imaging. An overall schematic of the fabrication of the D4 assay chip is shown in Fig. 1*E* and consists of the following sequential steps: (*i*) SI-ATRP to grow ~50-nm-thick POEGMA brushes on the glass surface, (*ii*) followed by noncontact inkjet printing of the cAb from buffer and a fluorescently labeled dAb with a molar excess of an excipient, typically PEG.

D4 Detection of Human IgM/IgG from Fingerstick. We first sought to test the concept of the D4 POCT and chose the detection of human IgG and IgM as a test case, as both analytes are present at high concentration in blood and should thus be detected by the assay. Furthermore, detection of IgG and IgM in the same assay also allowed us to assess the feasibility of carrying out a multiplexed D4 assay. To test this concept, a POEGMA-coated glass slide was stamped with a wax grid to confine the sample to the active area of the chip containing an inkjet-printed Ab array (Fig. 2*A*). The detection mixture was printed as three outer rings of soluble dAb spots containing a mixture of mouse Cy-5-anti-human-IgG and/or mouse Cy-5-anti-human-IgM (dAbs with a different epitope against human IgG and IgM than the cAb), with linear PEG (molecular weight 116,000), an excipient that
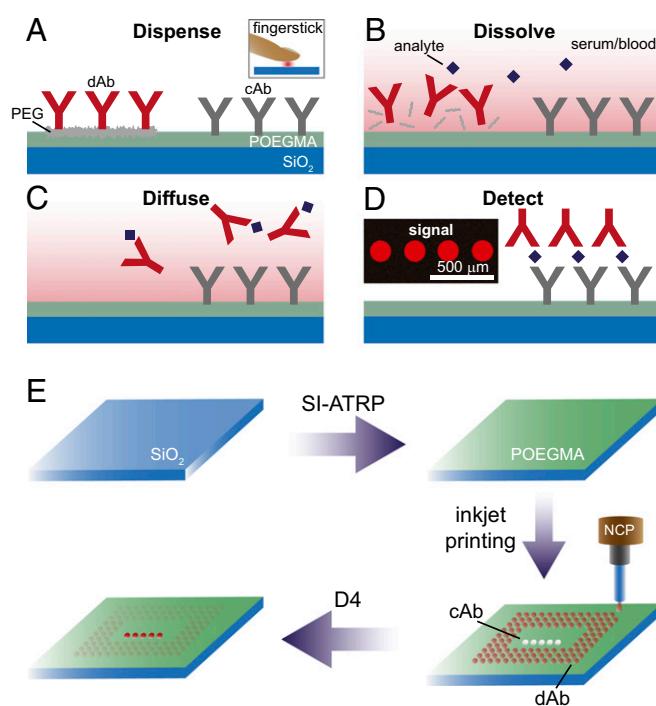

Fig. 1. D4 immunoassay on POEGMA brushes. (*A*) "Stable" spots of cAb and "soluble" spots of the fluorescently labeled dAb are printed onto the POEGMA brush. Whole blood or serum is dispensed directly onto the chip. (*B–D*) The sequence of events after addition of blood or serum is as follows. (*B*) "Soluble" dAb dissolves and binds to analyte. (*C*) These complexes diffuse and bind to their respective cAb spots, and subsequently (*D*) generate a quantifiable fluorescent signal. (*E*) D4 chip fabrication. Glass chips are coated with POEGMA with SI-ATRP. The cAb and detection reagents are spotted onto the surface with noncontact inkjet printing (NCP). After drying, chips are ready for use.

was added to enable dissolution of the dAbs upon contact with blood, and heparin to prevent coagulation of blood. The inner 4 × 4 array contains spots of "stable" cAb. Rows 1 and 4 are an anti-mouse cAb (positive control), row 2 is an anti-human IgG cAb, and row 3 is an anti-human IgM cAb.

Representative steps performed by a user are shown in Fig. 2 *B–D*. First, a drop of blood from a finger stick (Fig. 2*B*) is applied directly to the microarray and contained within the hydrophobic corral (Fig. 2*C*). After a predetermined incubation period (5 min for this experiment), the surface is rinsed with ~1 mL wash buffer from a squeeze bottle, which displaces the loosely bound blood cells and proteins (Fig. 2*D*). Interestingly, the blood flows to the margins and binds to the hydrophobic corrals, as seen from the red color around the margins in Fig. 2*D*, but is completely removed from the nonfouling POEGMA surface. The slide is then imaged with a fluorescence detector. The output of the D4 from a fluorescent scanner is shown in Fig. 2 *E–J*. Before exposure to blood, the inner 4 × 4 cAb array has no intrinsic fluorescence (Fig. 2*E*). Negative control experiments in which the D4 chip was incubated with either PBS (Fig. 2*F*) or whole chicken blood (Fig. 2*G*) show that only the positive-control spots (rows 1 and 4) generate signal, while middle rows 2 and 3 (specific for human IgG and IgM, respectively) show no fluorescence. Upon incubation with human blood with an array that is printed with a detection mixture of both Cy5-anti-human IgM and Cy5-anti-human IgG dAbs (Fig. 2*H*), rows 2 and 3 show positive fluorescence signal by "sandwiching" circulating human IgG (row 2) and IgM (row 3) analytes between a cAb and the Cy5-labeled dAb specific to each analyte. In contrast, when the outer dAb spots only contain Cy5-anti-human IgM dAb (Fig. 2*I*), only row 3 (IgM cAb) is
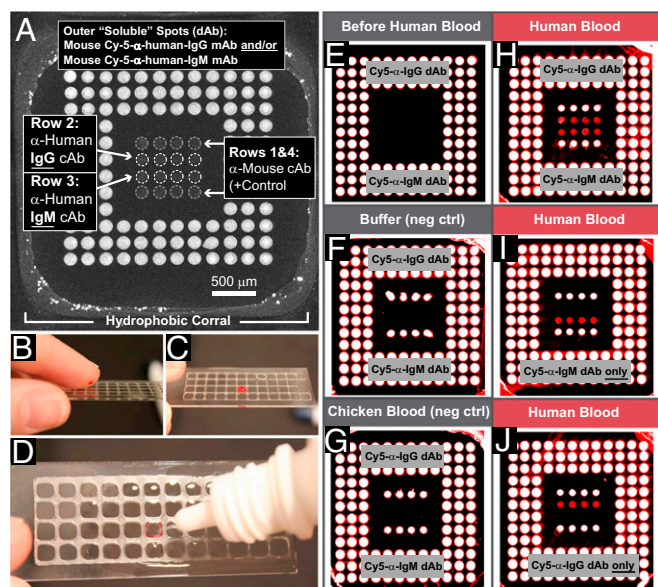
Fig. 2. D4 detection of human IgG and IgM from fingerstick blood. (*A*) D4 microarray within a single wax corral. Outer "soluble" dAb spots: murine Cy-5-anti(α)-human-IgG dAb and/or murine Cy-5-α-human-IgM dAb. Inner 4 × 4 "stable" cAb spots: α-mouse cAb as positive control (rows 1 and 4), α-human IgG cAb (row 2), α-human IgM (row 3). (*B–D*) Steps performed by use. (*B*) Application of fingerstick blood, (*C*) incubation for 5 min, and (*D*) washing with 1 mL of buffer from squirt bottle. (*E–I*) Results of D4 assay. (*E*) Before liquid exposure. (*F* and *G*) After exposure to PBS and whole chicken blood. (*H–J*) Results after adult human fingerstick blood (5 min). Each outer spot contains a mixture of PEG excipient, heparin, and (*H*) both Cy5-α-human-IgG and Cy5-α-human-IgM dAbs, (*I*) only Cy5 α-human-IgM dAb, or (*J*) only Cy5-α-human-IgG dAb.

visible but not row 2 (IgG cAb). The converse is true when the outer spots only contain Cy5-anti-human IgG dAb (Fig. 2*J*).

In summary, this proof-of-concept experiment demonstrated that printing both cAb and dAb together on POEGMA coatings greatly simplifies the sandwich immunoassay by eliminating the multistep procedures typically used in standard ELISA. It also suggested that multiplexed detection should be possible with the D4 assay, a desirable feature that has been historically difficult with LFIAs (16).

Quantitative Single-Analyte D4. The concentration of total Ig is relatively high in whole blood [approximately in the micromolar range (17)], so we next sought to examine the quantitative response of the D4 assay for analytes that occur at lower concentrations in complex biological matrices such as serum and whole blood. Fig. 3*A* shows representative image data of a D4 assay for the cytokine IL-6 exposed to whole chicken blood with and without spiked analyte (right and left panels, respectively). Similar to the array design in Fig. 2, soluble spots of anti–IL-6 dAb are printed as outer rings surrounding centrally located capture spots of anti–IL-6 cAb. These anti–IL-6 cAb spots were printed alongside spots of vehicle control (PBS) and positive-control capture spots (labeled "ctrl") comprised of anti-dAb Abs targeting the Fc portion of dAbs. These positive-control spots not only indicate whether dAbs were successfully localized to the active area of the assay but also help quantitatively correct for interassay variation as calibration spots (*SI Appendix*, Fig. S1). The images in Fig. 3*A* show minimal background signal, due to the nonfouling polymer brush, near-zero signal from anti–IL-6 cAb spots in the absence of analyte, and brightly fluorescent anti–IL-6 cAb spots in the presence of human IL-6–spiked blood. As expected, D4 signal was absent from vehicle control and brightly

fluorescent in positive-control spots in both cases. By measuring the fluorescence emission from cAb spots across a range of different concentrations in IL-6–spiked serum and whole blood (Fig. 3*B*), we obtained the dose–response curves shown in Fig. 3 *C* and *D*. For this IL-6–D4 assay, we calculated that the LODs in serum and blood were approximately 6.3 pg/mL and 10.9 pg/mL, which correspond to ∼310 and 536 fM, respectively, with a dynamic range spanning greater than three orders of magnitude [details for calculating figures of merit (FOM) are provided in *Materials and Methods*].

The D4 is a flexible platform for rapid immunoassay development. By inkjet printing spots of stable cAb and soluble dAb for various targets onto POEGMA-coated chips in a layout like that of Fig. 3*A* we were able to develop D4 chips for a variety of different markers. To demonstrate this versatility, in *SI Appendix*, Fig. S2 we show the performance of D4 immunoassays pertinent to oncology [prostate-specific antigen (PSA) and alpha-fetoprotein (AFP)], endocrinology (leptin), cytokine profiling (TNFα and IL-6), cardiology [B-type natriuretic peptide (BNP)], and infectious disease (HIV p24), in both serum and whole blood. The quantitative FOM for each analyte are summarized in Table 1. The data show that for each analyte tested the D4 is quantitative and sensitive with LODs that range from approximately 6.3 to 113 pg/mL, dynamic ranges between 2.3 to 3.9 orders of magnitude, and acceptable intra- and interassay coefficients of variation (COV$_{intra}$ and COV$_{inter}$; no greater than 15% and 20%, respectively). While the assays in Table 1 used incubation times of 90 min to maximize sensitivity, we observed that much shorter times can be used for sensitive assay readout. To examine the effect of incubation time on LOD, we carried out a leptin-D4 assay for incubation times ranging from 15 min to 90 min and found that the LOD only increased to 57 pg/mL for a D4 assay carried out for 15 min compared with 38 pg/mL for an assay carried out for 90 min (*SI Appendix*, Fig. S3).

An important design feature that we also considered in our implementation of the D4 was accounting for variability in factors such as sample volume and dissolution efficiency of soluble dAb, which may impact signal quantitation. Our approach to do so is described in greater detail in *SI Appendix*. Briefly, however,
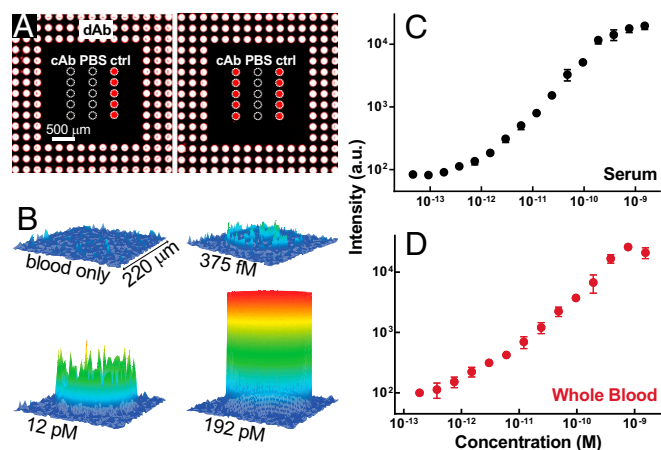
Fig. 3. Representative D4 against IL-6 in whole serum and blood. (*A*) D4 image data. Spots of Cy5-dAb against human IL-6 are printed around spots of anti–IL-6 cAb. Spots of PBS and anti-dAb Abs printed nearby serve as negative and positive controls, respectively. All spots are artificially outlined by a dashed white line to aid visualization of spot locations. Images show arrays exposed to whole chicken blood alone (*Left*) and blood spiked with IL-6 (*Right*). (*B*) Spatial intensity plots of fluorescence from individual cAb spots at various concentrations of IL-6 spiked in whole chicken blood. (*C* and *D*) Dose–response curves of IL-6 in (*C*) calf serum and (*D*) chicken blood. Each data point represents mean ± SD from three separately run D4 arrays. LODs in serum and blood were 6.3 and 10.9 pg/mL, respectively.

Table 1. D4 assay FOM

| Analyte	LOB, pg/mL	LOD, pg/mL	COV$_{intra}$, %	COV$_{inter}$, %	DR, log$_{10}$
AFP					
Calf serum	20.1	47.5	4.7	14.5	2.7
Chicken blood	30.0	58.9	6.3	13.5	2.8
PSA					
Calf serum	54.4	82.8	5.5	10.5	2.7
Chicken blood	51.0	112.9	8.0	11.0	2.5
Leptin					
Calf serum	10.3	38.2	6.4	8.2	3.2
Chicken blood	10.4	44.3	4.8	13.4	3.1
BNP					
Calf serum	2.1	25.2	10.8	19.1	3.7
Chicken blood	8.7	28.2	8.9	15.2	3.3
IL-6					
Calf serum	3.8	6.3	7.6	10.0	3.4
Chicken blood	3.7	10.9	7.1	14.1	3.1
TNFα					
Calf serum	2.0	11.1	9.8	19.9	3.0
Chicken blood	24.3	54.2	7.4	18	2.3
HIV p24					
Calf serum	4.8	11.0	9.9	13.3	3.9
Chicken blood	3.1	16.5	9.1	15.6	3.4

the effect of these variations can be eliminated by incorporating positive control calibration spots comprised of anti-dAb Abs that target the Fc portion of dAbs that are printed in the center of the D4 arrays alongside anti-analyte cAb spots, as shown in the image data of Fig. 3A and *SI Appendix*, Fig. S1A. The data in *SI Appendix*, Fig. S1 show a significant reduction in interassay variability upon normalization of the cAb spot intensity to the fluorescence intensity of control spots, and the normalized signal intensities are consistent across a range of sample volumes from 50 to 150 μL.

Quantitative Multianalyte D4. We next assessed the performance of the D4 assay to simultaneously quantify multiple biomarkers using an approach similar to that shown in Fig. 2. Printing spatially distinct capture spots on a 2D surface enables the detection of multiple targets from a single chip with the same fluorescent reporter. As a proof-of-concept demonstration, we developed duplexed assays against cytokine markers TNFα and IL-6 (Fig. 4) and cancer markers AFP and PSA (*SI Appendix*, Fig. S4). Fig. 4A shows an image of the multiplexed D4 against cytokines TNFα and IL-6 after incubation with analyte-negative chicken blood and indicates the location of capture spots and Cy5-labeled detection reagents. In a format similar to that of the single-analyte assays shown earlier, labeled detection reagents containing dAb for TNFα and IL-6 were printed in the region surrounding cAb spots.

As shown in Fig. 4B, performing the D4 in whole blood spiked with a mixture of both TNFα and IL-6 shows detectable fluorescence at both cAb spots for each analyte, in a dose-dependent manner, similar to that of the single-analyte assays shown in *SI Appendix*, Fig. S2. In contrast, Fig. 4 C and D show that when the multiplexed assays are exposed to either TNFα or IL-6 alone only cAb spots specific to each respective analyte show dose-dependent fluorescence. Similar multiplexed data for AFP and PSA are shown in *SI Appendix*, Fig. S4.

Pilot Clinical Study with D4. We next sought to test the D4 in human patients using a biomarker that would be useful for POC applications. From the panel of analytes shown in Table 1 we elected to test the performance of a D4 against leptin in a clinical setting. This choice was motivated by a recent study in Uganda by investigators at Duke University and Mulago Hospital which determined that a low serum leptin level (even below 50 pg/mL)

is a major biochemical risk factor predicting infant mortality due to malnutrition (18). The authors of this study suggested that leptin measurements could be used to identify and provide targeted treatment to malnourished children at highest risk of death. Unfortunately, many low-resource settings lack the infrastructure to perform hormone assays at such sensitivities and require blood specimens to be transported to larger facilities, which delays potentially life-saving treatment. We therefore speculated that the D4 may provide a useful diagnostic alternative to hormone assays carried out in a centralized laboratory by allowing sensitive and quantitative on-site leptin measurements.
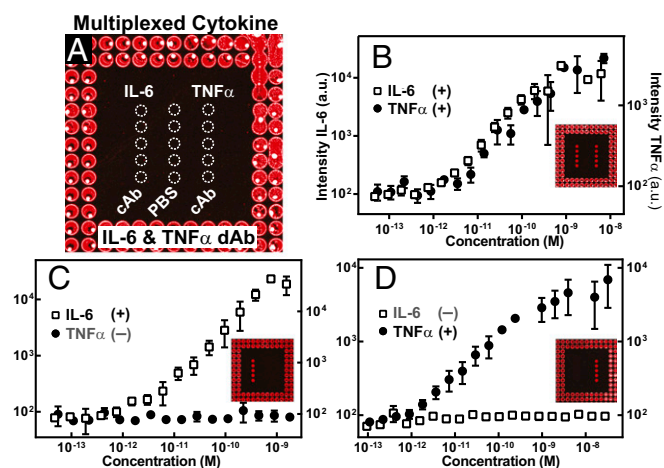
Fig. 4. Multiplexed assays against cytokine markers in whole blood. Fluorescent detection reagents against both analytes are coprinted as outer spots. Spots of cAb against IL-6 and TNFα are printed in the center of the array. (A) D4 image after incubation with whole chicken blood alone (without analyte). For clarity, spots for cAb and PBS are indicated with white dotted lines. (B) Dose–response curves after exposure to whole chicken blood spiked with a mixture of both IL-6 and TNFα analytes at varying concentrations. (C and D) Dose–response curves when assay exposed to varying concentrations of (C) IL-6 only or (D) TNFα only. Insets for panels B–D show D4 image data. Each data point represents mean ± SD from three separately run D4 arrays.
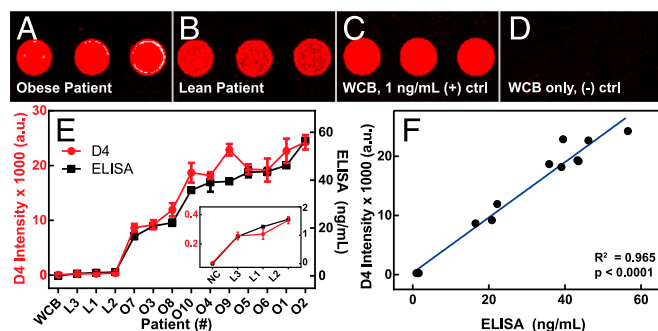
Fig. 5. Pilot clinical studies using D4 to measure leptin levels in pediatric patients. (*A–D*) Representative D4 imaging of whole blood specimens from an (*A*) obese patient and (*B*) lean patient immediately after blood draw. For comparison, D4 data of (*C*) whole chicken blood (WCB) spiked with 1 ng/mL human leptin (*D*) and human leptin-negative chicken blood alone are also shown. (*E*) D4 fluorescence readout compared with results from standard sandwich immunoassay in all patients. D4 data are shown in red and sandwich immunoassay data in black. (*Inset*) Zoomed graph of lean patients alone (NC = negative control serum). (*F*) Plot showing correlation between D4 versus sandwich immunoassay (R-squared = 0.965; *P* < 0.0001, two-tailed *t* test).

As proof of concept, we conducted a small IRB-approved pilot study at Duke University Medical Center (DUMC) comparing serum leptin levels detected by the D4 assay versus clinical ELISA from 3 lean [body mass index (BMI) <10%] and 10 obese (BMI 83.9–99.58%) pediatric patients. We selected this patient population to clinically test the D4 assay across a wide range of leptin levels, as serum leptin levels are proportional to adipose mass (19, 20). Our pilot studies demonstrated high concordance between D4 and clinical ELISA (Fig. 5). Fig. 5*A* shows D4 images from a representative obese and lean patient in whole blood, immediately after blood draw. The obese patients exhibited higher fluorescence intensities (indicating higher leptin levels) than lean patients (Fig. 5*B*), which is consistent with known adipocytokine physiology. Significantly, we found that the leptin levels measured by D4 correlated strongly with those measured by clinical ELISA performed in parallel in a central laboratory at DUMC across all 13 patients (*P* < 0.0001) (Fig. 5 *E* and *F*).

The readout of D4 microarray chips shown thus far was obtained using a sensitive table-top fluorescence scanner to assess the sensitivity of the D4 assay. While this approach would allow for POC testing in a peripheral laboratory near or attached to a clinic in LRSs (21), we recognize that a table-top scanner is too burdensome for use in the field. To address this issue, we next investigated the feasibility of portable fluorescence imaging of the D4 assay using a mobile phone-based fluorescence microscope (Fig. 6 and *SI Appendix*, Fig. S5). This apparatus is a compact and cost-effective imaging system that uses an external lens, in addition to the existing lens of the mobile phone camera (22, 23). The illumination is introduced at an oblique illumination angle of ~75° to increase the SNR of the acquired fluorescence images on the phone.

These experiments imaged leptin-D4 assays in both simulated and patient samples. For comparison, we also imaged the same set of D4 arrays (to maintain consistency) with the table-top scanner in the usual fashion. The fluorescence images in Fig. 6 *A* and *B* depict representative cAb spots of leptin-D4s (with and without analyte) using the table-top scanner and the mobile phone-based imager, respectively. In both cases, the fluorescence readout behaves as expected for leptin-spiked and leptin-deficient serum (left and right image panels), with good SNR. The dose–response curves using a dilution series of leptin-spiked calf serum are shown in Fig. 6 *A* and *B*. Both scanner and mobile phone-based imaging modalities showed quantitative, dose-dependent fluorescence intensities. In this experiment,

the scanner was more sensitive than the mobile phone, with LODs determined to be 0.037 ng/mL and 0.71 ng/mL, respectively. We next imaged a set of leptin-D4 arrays against clinical specimens obtained from obese patients in our pilot clinical study. The D4 readouts from the scanner (red trace) and from the mobile phone platform (blue trace) are shown in Fig. 6*C*. In both cases, as expected the data show good correspondence with ELISA values (dashed black trace).

Transitioning to the mobile phone-based detection platform reduced detection sensitivity and interassay consistency, as seen by the higher LOD and larger error bars with the mobile phone device. Nevertheless, these proof-of-concept studies demonstrate the feasibility of merging D4 assay technology with compact, field-portable, cost-effective, and easy-to-use mobile phone-based detection platforms. As mobile phone detector technology, computational imaging, and sensing approaches continue to evolve we expect that the fluorescence collection efficiency and hence sensitivity of these portable, low-cost detectors will rival table-top fluorescence scanners. Despite the lower sensitivity of this first-generation mobile phone detector, the field portability of mobile phone-based imaging provide a detection strategy that is well-matched to complement the robustness of the D4 assay technology with FOM that are sufficient for many clinical applications.
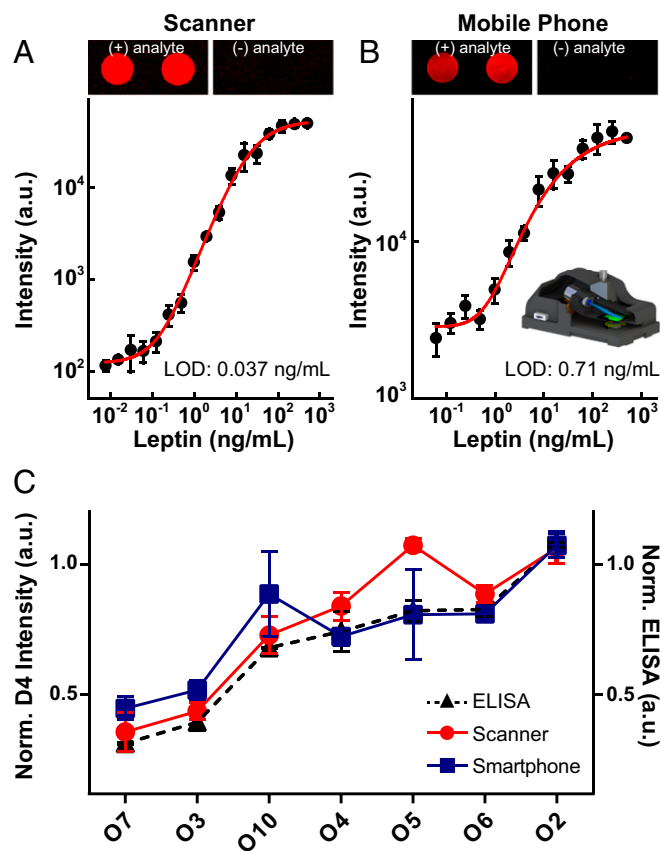
Fig. 6. Mobile phone-based imaging of D4 arrays. (*A* and *B*) Representative image data of D4 microspots and dose–response curves in calf serum spiked with leptin analyte acquired by a (*A*) benchtop scanner and (*B*) our mobile phone-based fluorescence microscope. Five-parameter logistic fit shown as red curve. (*B*, *Inset*) Illustration of the mobile phone attachment for fluorescence imaging and quantification of D4 arrays. (*C*) Testing of obese patient serum with D4 using a scanner (red trace) versus the mobile phone microscope (blue trace), and comparison with ELISA results (dashed black trace). Normalized D4 data (scanner, phone) plotted on the left axis, and normalized ELISA data plotted on the right axis.

Storage Stability of D4. Because use of the leptin D4 POCT in LRSs would necessitate long-distance shipment of assay materials to sites around the world, an important issue that needed to be addressed is the need for a "cold chain" and the storage stability of D4 chips. We hence measured the performance of D4 chips targeting leptin at different time points and under elevated temperatures after chip fabrication. Fig. 7 compares dose–response curves of leptin-D4s exposed to analyte-spiked calf serum under different storage conditions. In Fig. 7A, vacuum-sealed packets containing leptin-D4 chips were stored 1–92 d under ambient conditions. The data showed no significant difference in assay performance. Likewise, we also observed minimal difference in assay performance when vacuum-sealed chips were stored at 45 °C for up to 120 h (5 d) (Fig. 7B).

Discussion

The D4 POCT offers a promising platform for democratizing access to sensitive and quantitative assessment of diagnostic protein biomarkers. We first showed proof-of-concept application of multiplexed detection of human immunoglobulins. We observed ELISA-like performance across a wide range of protein analytes when assayed in unmodified serum and blood and showed the feasibility of quantification for multiple analytes from the same chip. Our pilot validation studies showed high concordance between D4 and ELISA in human patients, suggesting that this platform may ultimately be translatable to the clinical setting. Next, we introduced the feasibility of combining D4 chip technology with sensitive and cost-effective mobile phone readout for truly distributed use of the platform. Finally, the D4 chips showed durable storage stability, as evidenced by acceptable assay performance following exposure to heat or prolonged storage.

Much work has been previously done toward developing POCT platforms for LRSs. An "active" approach is to incorporate a fluid handling system where the reagents are stored on the device separately and then mixed and washed using pumps and valves, or alternatively by mechanisms that are conceptually similar but with smaller microfluidic devices (7, 24–27). This pioneering design strategy has seen commercial success in some embodiments (e.g., Abbott i-Stat) and shown encouraging field performance in others (26, 27). However, such systems have many parts, which increases the complexity and cost, and the finite possibility of malfunction from each individual component can limit the robustness of the device.

To date, "passively" driven immunoassays have experienced the most success as POCTs for protein analyte detection. LFIAs—the most widely used embodiment in LRSs—use nitrocellulose strips impregnated with dried capture/detection reagents that are passively colocated by applying liquid; this design permits a low-cost, rapid approach to protein detection in a user-friendly manner (fluid application with or without premixing, sometimes followed by buffer addition step and/or signal amplification) (5, 28). Despite

its strengths, the LFIA is not a substitute for the ELISA for two major reasons. First, LFIAs provide semiquantitative or qualitative readouts (in the absence of a dedicated reader), while conventional ELISA provides quantitative results with high accuracy and precision. Second, most LFIAs are not as sensitive as ELISA (29–31), as more antigen-antibody (Ag–Ab) interactions are necessary to generate a positive signal. This leads to certain clinical scenarios in which LFIA technology is unable to meet the required sensitivity to be practically useful (32). Furthermore, PBDs have been groundbreaking in further evolving passively driven devices for use in LRSs and offer many advantages over existing POCTs for their low cost, disposability, and ability to be assembled into multidimensional structures (33, 34). While a frequently encountered shortcoming with PBDs has been limited sensitivity, several innovative signal amplification techniques that reduce detection limit without significantly compromising usability have been described, most notably those using paper networks for automated sequential reagent delivery (12, 15) and enzymatic amplification (35). Such advances have made PBDs a promising platform for "lab-on-a-chip" diagnostics; however, more work remains toward addressing issues such as controlling the consistency of paper matrices, the underlying need for the sequential delivery of reagents and/or washing, challenges with multiplex analysis, and further improving detection sensitivities (34, 36). In contrast, capillary-driven PMFs (e.g., MBio and Philips Minicare) have overcome challenges in sensitivity faced by LFIAs and PBDs while retaining ease of use, with some platforms reaching subpicomolar LODs within 15 min (7, 37–42). By eliminating "active" elements (e.g., pumps), PMFs reduce the complexity and cost of microfluidic-based designs and significantly reduce instrumentation footprint compared with standard assays. While PMFs show great promise, challenges remain in further reducing instrumentation footprint and/or lowering cost of readers to fulfill the accessibility and sustainability requirements that are critical for successful dissemination and implementation in LRSs.

Our contribution toward democratizing accesses to clinical diagnostics—the D4—builds upon, but also departs significantly from, the accomplishments of existing "passive" POCT designs such as LFIAs, PBDs, and PMFs. The POEGMA interface is the critical element responsible for the high performance and simplicity of the D4. In the D4, the POEGMA brush is nonfouling in its hydrated state. The hydrated POEGMA brush virtually eliminates nonspecific binding of cells, proteins, and other biomolecular noise (8, 9, 43), yielding high SNRs even at low analyte concentration in complex matrices such as blood and obviates the need for microfluidic separation (preprocessing) of cells.

In the dry state, however, the POEGMA brush readily entraps Abs that are inkjet-printed into the polymer brush. Printing cAbs onto the dry brush without excipient leads to their stable immobilization within the brush and prevents bleeding or dissolution of cAb spots upon hydration with biological matrix (8). This leads to uniform capture spot morphology, which facilitates quantification and analysis. In contrast, printing detection reagents with an excess of soluble excipient onto the dry brush creates a reservoir for assay reagents. Contact with blood or other aqueous fluid causes dissolution of the excipient in printed spots of the dAb and releases the dAb from the chip, and the released dAb freely diffuses across the surface and drives the assay to completion. The direct inkjet printing of reagents onto POEGMA brush is another key element of the D4 assay, as it allows precise control over assay geometry, spot concentration, and composition, without the need for covalent coupling steps, which simplifies assay fabrication. Like many existing "passive" designs, the D4 stores all necessary reagents on the same device, but it does so by inkjet printing capture and detection reagents in very close proximity onto a nonfouling polymer brush. This design eliminates the need to control fluid movement with fluidics or include sequential liquid transfer steps. Combined, these features
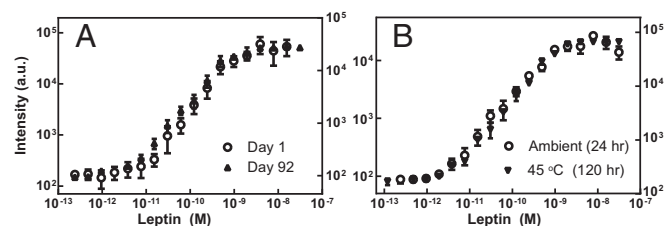
Fig. 7. Storage stability of the D4. Leptin-D4 chips were stored in vacuum-sealed packets under the conditions described and then run in analyte-spiked calf serum. (A) Dose–response curves for leptin-D4 after 1 d (○) and 92 d (▲) of storage in ambient temperature show similar performance. (B) Dose–response curves for leptin-D4 after 24 h of ambient storage versus 120 h (5 d) of storage at 45 °C show similar performance.

of the D4 platform translate to a robust, self-contained, and quantitative POCT without compromising assay performance or cost.

The low-cost fabrication of the D4 and smartphone-based reader, coupled to its sensitivity and quantitative performance, may offer a scalable and sustainable route to manufacturing multiplexed immunoassays for LRSs that are both affordable and analytically robust. When produced in bulk, we estimate that D4 chips would cost <$1 each (*SI Appendix*, Table S1) and the 3D-printed mobile phone attachment would cost <$30 each. In terms of workflow, we envision that the D4 platform can provide a streamlined protocol for protein analyte detection in both healthcare and research settings and can expand the capabilities of both. The ability to achieve multiplexed results with ELISA-like sensitivity after a single incubation/rinse step and without blocking greatly simplifies protein quantification, reduces time to results, and ultimately lowers costs. Admittedly, creating a multiplexed test in LFIA format is also relatively straightforward as it involves spotting multiple capture reagents onto a strip or adding additional test "lines." However, the LFIA is highly dynamic, as its constituents are constantly changing at a given location across a test strip and never fully equilibrate. Subsequently, assay readout relies on binding kinetics specifically during which reactants are sufficiently close to interact on a molecular level, and this varies for each individual test. Unless each test is isolated from the others, the same assay condition (e.g., running buffer, porous membrane, and flow rate) is applied to all tests, and one set of conditions is often not optimal for the multiple analytes of interest. While isolation of individual tests is not overly difficult and various strategies to this end are available (44), this adds to complexity of sample handling and cost. In contrast, the design of the D4 assay—by effectively colocalizing the detection and capture reagents and relying on 2D diffusion and equilibration "above" a nonfouling polymer brush—allows multiplexing without significantly increasing the assay complexity.

Difficulty in storage is a major factor restricting the implementation of laboratory-based tests in LRSs. We speculate that the storage stability of D4 is related to the high oligo(ethylene glycol) density of the POEGMA "bottle brush," which provide a protective environment that stabilizes the printed proteins against denaturation (8, 45). To put our results into context, LFIAs are already well-suited for LRSs since they are generally stable for 1 to 2 y at ambient temperature and 6 mo at elevated temperature (45 °C) (16), and similar reagent stability has also been shown in other POCTs (46, 47) . The timescales for storage stability used in our studies with the D4 (Fig. 7) were shorter than those determined for LFIAs. Thus, while encouraging, we recognize that further studies are required to characterize the storage limitations of the D4 and, if needed, modifying packing and/or printing solutions with existing methods for reagent stabilization (35, 48) to meet the storage demands of LRSs.

For patient care, we envision that this technology will provide a robust POCT that is widely applicable for the diagnosis of a disease by quantification of the levels of one or more markers for which orthogonal Ab pairs are available. In the developed world, this will bring highly sensitive immunoassays to first responders and to the bedside, while in LRSs it will allow them to simply become more routinely available. The low cost of the chips and detectors also suggests that wide dissemination of this technology is feasible, so that it would also provide new opportunities for spatiotemporal mapping and remote analysis of measurement results, which would be highly valuable for epidemiology in general. However, it is worthwhile to note that the actual need for ELISA-like sensitivities depends on the disease and biomarker, which must be considered when deciding between the D4 POCT and other robust alternatives such as LFIAs or PBDs when such sensitivities are not required.

There are several challenges that still need to be resolved. The first is the requirement to remove the blood from the chip before imaging. Because proteins do not adsorb to the POEGMA brush surface and cells similarly do not adhere and are only settled on to the surface by gravity, removal of the blood from the chip is currently easy to perform using a buffer rinse. We acknowledge, however, that the open wash requirement is not ideal for biosafety reasons and possible specimen contamination. The ability to read out the assay in a sealed system with an automated wash or even in the presence of blood would make this a completely hands-off POCT, which is desirable. We are currently pursuing several solutions to this problem, including a PMF-based enclosed chip design that passively removes the blood before readout, as well as electronic modes of detection where the blood does not interfere with the signal, which will be reported separately. The second issue is the sensitivity of the fluorescence detector. While the current design of the cell phone detector is sensitive enough for many clinical applications, we believe that optimization of the detector design will yield the necessary 10- to 20-times improvement to match the performance of table-top fluorescence scanners that are the "gold standard" for imaging microarrays. This assessment is supported by reports of mobile phone-based fluorescence imaging of individual fluorescent nanoparticles and viruses (22) and fluorescently labeled single DNA molecules (23). Third, while the ubiquitous nature of mobile phones makes it a promising platform for dedicated and nondedicated POCT platforms, there will be challenges with effectively integrating them into healthcare systems. A thorough discussion of this topic is provided in the review by Byrnes et al. (33), but in brief, issues related to developing protocols for transmitting and interpreting results and subsequently making management decisions from POC data must be resolved. Furthermore, the diversity of phone models and short life cycles in both hardware and software lead to challenges in compatibility and maintaining common standards; the slow pace of regulatory approval also introduces its own set of obstacles. However, these are challenges faced by the entire field of mobile phone-based diagnostics and are not limited to the D4 POCT. We believe the widespread dissemination of phones, their user friendliness, and their computing power make them very attractive vehicles toward democratizing access to gold-standard diagnostic testing. In conclusion, the D4 POCT, combined with the field portability of mobile phone-based imaging, may pave the way for high-performance and user-friendly diagnostic immunoassays that are virtually independent from infrastructural requirements.

Materials and Methods

SI-ATRP of POEGMA on SiO₂ Substrates. In brief, POEGMA surfaces were deposited by SI-ATRP, specifically using an activator regenerated by electron transfer approach under aqueous conditions (49, 50). The experimental conditions used to create POEGMA polymer brush coatings "grafted from" substrate surfaces for our experiment are described in extensive detail elsewhere (8). These methods involve first functionalizing the substrate surface with a bromide ATRP initiator and then immersing the substrates in polymerization solution, producing surface-tethered brushes of POEGMA ~50 nm thick.

Spotting of Antibody Microarrays. All capture/detection Ab pairs and Ag were obtained from R&D Systems. The dAbs were directly conjugated to fluorophores per the manufacturer's instructions. The cAbs (1 mg/mL) were spotted onto POEGMA-coated substrates using a PerkinElmer Piezorray noncontact printer under ambient conditions at 1 mg/mL concentration. Spots of soluble detection reagents were composed of dAbs (1 mg/mL) mixed with excipient (1 mg/mL PEG 115,000 or 0.25 mg/mL trehalose) and printed in a similar fashion. For experiments using fingerstick blood (Fig. 2), spots of heparin were also included in arrays to maintain anticoagulation. After printing, D4 chips were placed under vacuum dessication (30 KPa) overnight to facilitate noncovalent immobilization of Abs into the polymer brush.

D4 Immunoassay. To generate dose–response curves, D4 chips were incubated with dilution series of analyte-spiked calf serum (Clontech) or whole chicken blood (Innovative Research, Inc.) for 90 min. Substrates were then

briefly rinsed in 0.1% Tween-20/PBS then dried. Arrays were imaged on an Axon Genepix 4400 tabletop scanner (Molecular Devices, LLC). The limit-of-blank (LOB) was estimated from the mean fluorescence intensity (μ) and SD (σ) from 10 blank samples, defined as LOB = μ_{blank} + 1.645σ_{blank}, as described by Armbruster and Pry (51). LOD was estimated from spiked low-concentration samples (LCS) above the LOB, such that LOD = LOB + 1.645σ_{LCS}. Low, intermediate, and high concentrations within the working range of each assay were used to determine the COV$_{intra}$ and COV$_{inter}$. The dynamic range (DR) was defined as the range of concentrations from the LOD to the greatest concentration that had a fluorescence signal greater than 3σ of that from the next-lower concentration in the dilutions series. Data were fit to a five-parameter logistic (5-PL) fit curve (52) using OriginPro 9.0 (OriginLab Corp.). Details on the effect of shorter incubation times (15 min and 60 min) on assay results are shown in *SI Appendix*, Fig. S2.

D4 and ELISA Measurements of Patient Leptin. Approval for clinical studies was obtained from the Duke University Health System Institutional Review Board (protocol no. Pro00064838). Parental assent and subject assent were first obtained, and then 0.5–1.0 mL of blood was drawn in a lavender-top collection tube containing K2-EDTA. For D4 assays in whole blood the blood was directly applied to D4 chips immediately after collection then processed and analyzed as usual. For D4-sandwich immunoassay comparisons the tube was then centrifuged for 10 min at 1,500 × *g*, and the resulting serum was aliquoted into cryovials and stored at −80 °C for later use. Samples were then thawed and analyzed with D4 and ELISA in parallel. Standard leptin sandwich immunoassays (Quantikine ELISA kit; R&D Systems) were performed per the manufacturer's instructions, which required a 100× dilution with assay diluent buffer for all specimens. For D4 measurements, specimens from lean patients were directly run without dilution. In contrast, we found that two obese patient specimens had extremely high leptin levels, above the upper limit of quantitation of the leptin D4. Thus, all specimens from obese patients (to maintain consistency) were diluted 10× with whole calf serum (and not sandwich immunoassay diluent buffer, to effectively maintain complexity of the biological milieu) before running the leptin D4.

Mobile-Phone Imaging of D4 Arrays. The mobile phone-based D4 assay reader device was created by integrating a 3D-printed optomechanical attachment to a smartphone (Lumia 1020; Nokia) which included an oblique illumination source for highly sensitive fluorescence detection (*SI Appendix*, Fig. S5) (22, 23). A standard microscope slide can be inserted into the smartphone at-

tachment from the side and illuminated by an excitation beam from a battery-powered laser diode (638 nm, 180 mW; Mitsubishi Electric) at an incidence of ~75° from the back side (*SI Appendix*, Fig. S5A). The fluorescence signal of the sample was collected from the other side of the glass slide by an external lens (f_2 = 2.6 mm; UCTronics) and passed through an emission filter (690/50 nm; Semrock) before entering the smartphone camera unit (*SI Appendix*, Fig. S5A). The smartphone camera is equipped with a 2/3-inch complementary metal-oxide semiconductor sensor with 41 megapixels and 1.12 μm in pixel pitch. The default smartphone camera lens assembly (Carl Zeiss) has an effective focal length of f_1 = ~6.86 mm, and therefore the nominal magnification (M) of the smartphone-based fluorescence microscope is M = ~2.6× . This mobile microscope design provides a half-pitch resolution of ~0.98 μm over an imaging field of view of ~0.8 mm^2 as characterized earlier (53). The size of the device is about 14.5 × 8.0 × 7.8 cm in length, width, and height, respectively, and the weight of the attachment excluding the smartphone is ~185 g. For a typical fluorescence image, an integration time of 4 s was used on the mobile phone. Fluorescence images were initially saved in raw DNG format (7,152 × 5,368 pixels) on the phone memory and subsequently converted into 16-bit TIFF for further analysis. Image analysis and quantification were performed by ImageJ on a desktop computer for this study and can be conducted by a custom-developed smart application running on the same phone in future designs.

1. Drain PK, et al. (2014) Diagnostic point-of-care tests in resource-limited settings. *Lancet Infect Dis* 14:239–249.
2. Hay Burgess DC, Wasserman J, Dahl CA (2006) Global health diagnostics. *Nature* 444:1–2.
3. Urdea M, et al. (2006) Requirements for high impact diagnostics in the developing world. *Nature* 444:73–79.
4. Hu L, Xu G (2010) Applications and trends in electrochemiluminescence. *Chem Soc Rev* 39:3275–3304.
5. Posthuma-Trumpie GA, Korf J, van Amerongen A (2009) Lateral flow (immuno)assay: Its strengths, weaknesses, opportunities and threats. A literature survey. *Anal Bioanal Chem* 393:569–582.
6. Nilghaz A, Guan L, Tan W, Shen W (2016) Advances of paper-based microfluidics for diagnostics—The original motivation and current status. *ACS Sensors* 1:1382–1393.
7. Chin CD, Linder V, Sia SK (2012) Commercialization of microfluidic point-of-care diagnostic devices. *Lab Chip* 12:2118–2134.
8. Hucknall A, et al. (2009) Simple fabrication of antibody microarrays on nonfouling polymer brushes with femtomolar sensitivity for protein analytes in serum and blood. *Adv Mater* 21:1968–1971.
9. Ma H, Li D, Sheng X, Zhao B, Chilkoti A (2006) Protein-resistant polymer coatings on silicon oxide by surface-initiated atom transfer radical polymerization. *Langmuir* 22:3751–3756.
10. Selby C (1999) Interference in immunoassay. *Ann Clin Biochem* 36:704–721.
11. Krishnan S, Weinman CJ, Ober CK (2008) Advances in polymers for anti-biofouling surfaces. *J Mater Chem* 18:3405–3413.
12. Fu E, et al. (2011) Enhanced sensitivity of lateral flow tests using a two-dimensional paper network format. *Anal Chem* 83:7941–7946.
13. Liang T, et al. (2016) Investigation of reagent delivery formats in a multivalent malaria sandwich immunoassay and implications for assay performance. *Anal Chem* 88:2311–2320.
14. Schonhorn JE, et al. (2014) A device architecture for three-dimensional, patterned paper immunoassays. *Lab Chip* 14:4653–4658.
15. Fu E, Lutz B, Kauffman P, Yager P (2010) Controlled reagent transport in disposable 2D paper networks. *Lab Chip* 10:918–920.
16. O'Farrell B (2009) *Evolution in Lateral Flow-Based Immunoassay Systems* (Humana, New York).
17. Buckley CE, 3rd, Dorsey FC (1971) Serum immunoglobulin levels throughout the lifespan of healthy man. *Ann Intern Med* 75:673–682.
18. Bartz S, et al. (2014) Severe acute malnutrition in childhood: Hormonal and metabolic status at presentation, response to treatment, and predictors of mortality. *J Clin Endocrinol Metab* 99:2128–2137.
19. Considine RV, et al. (1996) Serum immunoreactive-leptin concentrations in normal-weight and obese humans. *N Engl J Med* 334:292–295.
20. Heptulla R, et al. (2001) Temporal patterns of circulating leptin levels in lean and obese adolescents: Relationships to insulin, growth hormone, and free fatty acids rhythmicity. *J Clin Endocrinol Metab* 86:90–96.
21. Pai NP, Vadnais C, Denkinger C, Engel N, Pai M (2012) Point-of-care testing for infectious diseases: Diversity, complexity, and barriers in low- and middle-income countries. *PLoS Med* 9:e1001306.
22. Wei Q, et al. (2013) Fluorescent imaging of single nanoparticles and viruses on a smart phone. *ACS Nano* 7:9147–9155.
23. Wei Q, et al. (2014) Imaging and sizing of single DNA molecules on a mobile phone. *ACS Nano* 8:12725–12733.
24. Gervais L, de Rooij N, Delamarche E (2011) Microfluidic chips for point-of-care immunodiagnostics. *Adv Mater* 23:H151–H176.
25. Linder V (2007) Microfluidics at the crossroad with point-of-care diagnostics. *Analyst (Lond)* 132:1186–1192.
26. Chin CD, et al. (2011) Microfluidics-based diagnostics of infectious diseases in the developing world. *Nat Med* 17:1015–1019.
27. Laksanasopin T, et al. (2015) A smartphone dongle for diagnosis of infectious diseases at the point of care. *Sci Transl Med* 7:273re271.
28. O'Connor TP (2015) SNAP assay technology. *Top Companion Anim Med* 30:132–138.
29. Linares EM, Kubota LT, Michaelis J, Thalhammer S (2012) Enhancement of the detection limit for lateral flow immunoassays: Evaluation and comparison of bioconjugates. *J Immunol Methods* 375:264–270.
30. Gordon J, Michel G (2008) Analytical sensitivity limits for lateral flow immunoassays. *Clin Chem* 54:1250–1251.
31. Rifai N, Gillette MA, Carr SA (2006) Protein biomarker discovery and validation: The long and uncertain path to clinical utility. *Nat Biotechnol* 24:971–983.
32. St John A, Price CP (2014) Existing and emerging technologies for point-of-care testing. *Clin Biochem Rev* 35:155–167.
33. Byrnes S, Thiessen G, Fu E (2013) Progress in the development of paper-based diagnostics for low-resource point-of-care settings. *Bioanalysis* 5:2821–2836.
34. Yetisen AK, Akram MS, Lowe CR (2013) Paper-based microfluidic point-of-care diagnostic devices. *Lab Chip* 13:2210–2251.

35. Ramachandran S, Fu E, Lutz B, Yager P (2014) Long-term dry storage of an enzyme-based reagent system for ELISA in point-of-care devices. *Analyst (Lond)* 139: 1456–1462.

36. Liana DD, Raguse B, Gooding JJ, Chow E (2012) Recent advances in paper-based sensors. *Sensors (Basel)* 12:11505–11526.

37. Venge P, et al. (2017) Equal clinical performance of a novel point-of-care cardiac troponin I (cTnI) assay with a commonly used high-sensitivity cTnI assay. *Clin Chim Acta* 469:119–125.

38. Kemper DWM, et al. (2017) Analytical evaluation of a new point of care system for measuring cardiac Troponin I. *Clin Biochem* 50:174–180.

39. McGrath TF, et al. (2015) Development of a rapid multiplexed assay for the direct screening of antimicrobial residues in raw milk. *Anal Bioanal Chem* 407:4459–4472.

40. Logan C, et al. (2016) Rapid multiplexed immunoassay for detection of antibodies to Kaposi's sarcoma-associated herpesvirus. *PLoS One* 11:e0163616.

41. Broger T, et al. (2017) Diagnostic performance of tuberculosis-specific IgG antibody profiles in patients with presumptive tuberculosis from two continents. *Clin Infect Dis* 64:947–955.

42. Lochhead MJ, et al. (2011) Rapid multiplexed immunoassay for simultaneous sero-diagnosis of HIV-1 and coinfections. *J Clin Microbiol* 49:3584–3590.

43. Ma HW, Hyun JH, Stiller P, Chilkoti A (2004) "Non-fouling" oligo(ethylene glycol)-functionalized polymer brushes synthesized by surface-initiated atom transfer radical polymerization. *Adv Mater* 16:338–341.

44. Li J, Macdonald J (2016) Multiplexed lateral flow biosensors: Technological advances for radically improving point-of-care diagnoses. *Biosens Bioelectron* 83:177–192.

45. Michel R, Pasche S, Textor M, Castner DG (2005) Influence of PEG architecture on protein adsorption and conformation. *Langmuir* 21:12327–12332.

46. Anderson GP, et al. (1994) Development of an evanescent wave fiber optic biosensor. *IEEE Eng Med Biol Mag* 13:358–363.

47. Chan CP, et al. (2013) Evidence-based point-of-care diagnostics: Current status and emerging technologies. *Annu Rev Anal Chem (Palo Alto, Calif)* 6:191–211.

48. Ohtake S, Wang YJ (2011) Trehalose: Current use and future applications. *J Pharm Sci* 100:2020–2053.

49. Simakova A, Averick SE, Konkolewicz D, Matyjaszewski K (2012) Aqueous ARGET ATRP. *Macromolecules* 45:6371–6379.

50. Jakubowski W, Matyjaszewski K (2006) Activators regenerated by electron transfer for atom-transfer radical polymerization of (meth)acrylates and related block co-polymers. *Angew Chem Int Ed Engl* 45:4482–4486.

51. Armbruster DA, Pry T (2008) Limit of blank, limit of detection and limit of quanti-tation. *Clin Biochem Rev* 29:S49–S52.

52. Gottschalk PG, Dunn JR (2005) The five-parameter logistic: A characterization and comparison with the four-parameter logistic. *Anal Biochem* 343:54–65.

53. Kühnemund M, et al. (2017) Targeted DNA sequencing and in situ mutation analysis using mobile phone microscopy. *Nat Commun* 8:13913.

CHILKOTI, ASHUTOSH, Ph.D.

Changes:
Grants Ended: North Carolina Biotechnology Center grant—ended 9/30/17; Pfizer grant—ended 9/11/17
New Grants: USAMRAA SO150005, W81XWH-16-C-0219; NIH, 1R01GM123542; Dr. Reddy's Laboratories—2 new grants (CIS-Platinate and Paclitaxel); NIH, UG3CA211232; NIH, 1R21CA218940; NSF, 1729671; USAMRMC, DM160400

Active

Title: Center for Environmental Implications for Nanotechnology (PI – Wiesner)
Supporting Agency: National Science Foundation NSF-EF-0830093
Time Commitment: 0 Adacemic/0.2 Summer (~1.6% effort)
Performance Period: 9/15/03 – 8/31/18
Level of Funding: $20,890 (Annual Direct)
Grant Officer: Irwin Forseth, iforseth@nsf.gov, 703-292-7862
Goals and Specific Aims: The proposed Center explores the role of nano-scale phases in ecosystems, their interactions with organisms, and the mechanisms by which they exert their influence. The Center will translate this knowledge into the language of risk assessment /to provide guidance in interpreting the role of anthropogenic sources of nanomaterials and their relative impacts.

Title: Elastin Fusion Proteins
Supporting Agency: NIH/NIGMS 2R01 GM061232
Time Commitment: 1 Academic (~8.3% effort)
Performance Period: 4/1/00 – 6/30/18
Level of Funding: $209,349 (Annual Direct)
Grant Officer: Dina Wilson, dina.wilson@nih.gov, 301-594-9251
Goals and Specific Aims: The overall objective of this competing R01 application is to discover new peptide motifs that seamlessly encode both lower critical solution temperature (LCST) phase behavior and bioactivity, and to use these new sequences to create the "next-generation" of LCST polymers with intrinsic biological activity and self-assembled structures with morphological diversity and enhanced stability.
Specific Aim 1: Characterize the sequence space of Pro- and Gly-containing motifs that polymerize into LCST peptide polymers.
Specific Aim 2: Investigate the self-assembly of LCST block copolymers that exhibit hysteretic phase behavior into kinetically stabilized nano-mesoscale structures.
Specific Aim 3: Create LCST peptide polymers with intrinsic biological function.
Specific Aim 3**:** Carry out in vivo efficacy studies of a subset of PODs from SA2 to determine the long-term therapeutic potential of GLP-1 PODs.

Title: Collaborative Research: Supramolecular Materials by Nucleic Acid Block Copolymer Self-Assembly
Supporting Agency: National Science Foundation DMR-14-11126
Time Commitment: .0.05 Summer (~0.4% effort)
Performance Period: 7/15/14 – 6/30/18
Level of Funding: $390,000 (Total Project Cost)
Grant Officer: Elizabeth Gebremendhin, (703) 292-4444
Goals and Specific Aims: The overall goal of this interdisciplinary, collaborative research proposal is to design and synthesize polynucleotide (co)polymers with chemical functionalities that drive solution self-assembly into

micelles and that harness DNA's molecular recognition properties to create oriented, supramolecular polynucleotide networks over large areas on surfaces.

Title: Treating Melanoma with a Molecularly Engineered, Long Circulating Immunotoxin
Supporting Agency: NIH 1R21-EB019041
Time Commitment: 0.24 Academic (~2% effort)
Performance Period: 9/15/2015 – 6/30/2018
Level of Funding: $125,000 (Annual Direct)
Grants Officer: Angelos Bacas, ab329b@nih.gov, 301-451-4785
Goals and Specific Aims: The proposed research will develop a new bioengineered drug by InStealth polymer conjugation, in which a polymer that has long in vivo circulation and good tumor accumulation will be directly grown from the N- or C-terminus of a ―biologic‖ drug —a protein that consists of an antibody fragment that homes in on melanoma cells, and which is fused to a potent bacterial toxin that kills cells. We will demonstrate the utility of the InStealth™ technology in improving the treatment of melanoma by this polymer modified protein drug.

Title: Non-immunogenic PEG conjugates of Biologics
Supporting Agency: North Carolina Biotechnology Center
Time Commitment: 0.14 Academic (~1.2% effort)
Performance Period: 09/01/2016 - 02/28/2018
Level of Funding: $100,000
Grants Officer: Joan Pifer, joan_pifer@ncbiotech.org
Goals and Specific Aims: The outcome of the project will be the identification of a fully optimized exendin-POEMGA conjugate with minimal antigenicity, and a technology that provides a superior alternative to PEGylation, with application to the entire class of biologic drugs.

Title: SO150005: Smartphone Enabled Point-of-care Diagnostics for Operationally Significant Pathogens
Supporting Agency: USAMRAA, W81XWH-16-C-0219
Time Commitment: 0.9 academic months (~7.5% effort)
Performance Period: 9/28/16-9/27/18
Level of Funding: $343,575, total funding to date
Grants Officer: Benjamin Chitty, Benjamin.chitty@socom.mil, 813-826-5162
Goals and Specific Aims: The overarching goal of this project is to develop point-of-care tests (POCTs) against infectious diseases of operational significance, ready for large-scale validation against human samples.

Title: Magnetically directed single cell transcriptome analysis
Supporting Agency: NIH, 1R01GM123542
Time Commitment: 0.5 summer months (~4.2% effort)
Performance Period: 9/20/16-8/31/21
Level of Funding: $28,973 (Annual Direct, Chilkoti portion only)
Grants Officer: Jennifer Billington, billingj@nigms.nih.gov, (301) 594-5243
Goals and Specific Aims: Dr. Chilkoti will oversee the development of the immunoarray's POEGMA surface during the early years of the assay development. He will work closely with Dr. Yellen in optimizing the overall design of the chip to accomplish this goal and directly supervise staff during all steps of the process.

Title: Self-assembled microporous networks for cell culture
Supporting Agency: EMD Millipore
Time Commitment: 0.9 Academic months (~7.5% effort)
Performance Period: 5/1/17-4/30/19
Level of Funding: $200,000 (Annual Direct Costs)
Grants Officer: Martin Zillman, martinzillmann@emdmillipore.com

Goals and Specific Aims: Work on developing POP microcarriers will proceed on a two year, two-phase timeline. Phase one will be devoted to developing a reproducible microcarrier prototype capable of supporting cell growth and rapid dissolution for cell recovery.

Title: Delivery of paclitaxel by Recombinant Polypeptide Nanoparticles
Supporting Agency: Dr. Reddy's Laboratories, Ltd.
Time Commitment: 0.75 Academic months (~6.2% effort)
Performance Period: 3/30/17-3/29/18
Level of Funding: $393,000 (Total Project Costs)
Grants Officer: Ajaya Reka, areka@drreddys.com
Goals and Specific Aims: Our second goal is to design and test a "next-generation" nanoparticle that binds endogenous albumin, and thereby enhances the pharmacokinetics, biodistribution and tumor targeting ability of the ELP-PTX nanoparticle.

Title: Delivery of Cis-Platinate by Recombinant Polypeptide Nanoparticles
Supporting Agency: Dr. Reddy's Laboratories, Ltd.
Time Commitment: 0.75 Academic months (~6.2% effort)
Performance Period: 3/30/17-3/30/18
Level of Funding: $159,000 (Total Project Costs)
Grants Officer: Ajaya Reka, areka@drreddys.com
Goals and Specific Aims: The objective of this project is to develop two alternative methodologies to create cis-platinate loaded nanoparticles of a recombinant elastin-like polypeptide (ELP)

Title: Smartphone Enabled Point-of-Care Detection of Serum Markers of Liver Cancer
Supporting Agency: NIH, UG3CA211232
Time Commitment: 0.25 Academic month/1.15 Summer months (~11.6% effort)
Performance Period: 6/1/17-4/30/19
Level of Funding: $268,236 (Annual Direct Costs)
Grants Officer: Jo Ann S. Rinaudo, rinaudoj@mail.nih.gov, (240) 276-7133
Goals and Specific Aims: The overall goal of this R01 proposal is to develop a multiplexed point-of-care test (POCT) for serum markers of hepatocellular carcinoma (HCC), and to validate this POCT in the People's Republic of China, where the incidence of HCC is disproportionately high.

Title: Image-guided Dosimetry for Injectable Brachyterapy based on Elastin-like Polypeptide Nanoparticles
Supporting Agency: NIH, 1R21CA218940
Time Commitment: 0.67 Academic months (~5.6% effort)
Performance Period: 8/1/17-7/31/19
Level of Funding: $130,500 (Annual Direct Costs)
Grants Officer: Jacek Capala, capalaj@mail.nih.gov, (240) 276-5690
Goals and Specific Aims: The overall objective of this proposal is to provide critical infrastructure by developing, validating, and evaluating a methodology for determining optimal image-guided dosimetry for ELP-based injectable brachytherapy.

Title: DMREF: Collaborative Research: High throughput Exploration of Sequence Space of Peptide Polymers that Exhibit Aqueous Demixing Phase Behavior
Supporting Agency: NSF, 1729671
Time Commitment: 0.075 Summer months (~0.6% effort)
Performance Period: 10/1/17-9/30/21
Level of Funding: $1,183,788 (Total Project Costs)
Grants Officer: John Schlueter, (703) 292-7766

Goals and Specific Aims: The primary goal of the proposed research is to develop generalized materials design rules, by combining experiments, fast computer simulations and data science to accelerate the discovery and development of a potentially huge class of thermally responsive polypeptide materials. (1) Prediction of stimuli responsive behavior through machine–learning algorithms that are trained and validated by high throughout synthesis and characterization of LCST and UCST phase behavior; (2) Computational design and development of responsive 3-D polypeptide materials from building blocks from specific aim 1.

Title: A Point-of-Injury Screening Assay for Tactical Damage Control Resuscitation
Supporting Agency: USAMRMC, DM160400
Time Commitment: 1 Summer month (~8.3% effort)
Performance Period: 9/15/17-9/14/20
Level of Funding: $1,399,701 (Total Project Costs)
Grants Officer: Thomas Winter, Sidney.t.winter.civ@mail.mil, (240) 357-1590
Goals and Specific Aims: This proposal will develop a portable, ruggedized, handheld, and non-invasive test to be used at the point-of-injury to accomplish the following 3 tasks from a single drop of finger stick blood: blood type matching, infectious disease screening, and monitoring of lactate levels as a marker for trauma.